Optimization of a one-part geopolymerization method for lab-scale using waste glass wool as a precursor

Oscar Enander

Optimization of one-part geopolymerization method for lab-scale, using waste glass wool as a precursor

By

Oscar Enander

Department of Chemical Engineering
Lund university
&
Ecophon Saint Gobain
June 2022

Supervisor: Reine Wallenberg
Co-supervisor: Saleh Hooshmand
Examiner: Ola Wendt

Abstract

Geopolymers are amorphous inorganic polymeric structures. They are used as binding agents and can be compared to cementitious materials such as ordinary Portland cement. This thesis aims to produce geopolymers from waste glass wool. Today glass wool is found in isolation, both thermal and sound insulation, and it is not being recycled. Most of the glass wool waste ends in landfills. Studies have been conducted to ensure the viability of using glass wool as the main component in geopolymers. In this project, 80% of the binder is waste glass wool. The samples are produced using the one-part approach to the geopolymer reaction, this method makes for safer handling than the two-part approach. The samples are analysed using XRD, TGA, microscopy and compressive strength testing. The curing temperature influences the compressive strength with increasing compressive strength with temperature up to 60°C. The water to binder ratio contributes a lot to the strength of the geopolymer, a higher water to binder ratio gives a lower compressive strength. The amount of sodium silicate increases the compressive strength, the increase is found up to 21% of sodium silicate. Above 21% the strength increase subsides. The TGA shows that 10% of the weight of the sample after 28 days of drying in ambient temperature and humidity is water. It also shows changes in weight due to the phenolic binder used to coat the glass fibres. The highest compressive strength for geopolymers in this report is 55 MPa. This study shows that to optimize the production, the capability of the equipment and the application of the geopolymer needs to be taken into consideration.

Acknowledgement

I would like to thank a lot of people for the help and support during this thesis. I would like to thank Reine Wallenberg my supervisor at LTH. I would also like to thank my examiner, Ola Wendt. A special thanks are sent to my supervisor at Ecophon Saleh Hooshmand. You have helped me a lot throughout the project I would also like to thank Jennifer Von for the valuable discussions and the employees of the R&D department at Ecophon for the welcoming atmosphere. Lastly, I would like to thank my wife and my family and friend for the support while writing this thesis.

Populärvetenskaplig sammanfattning

Tänk om vi kunde minska utsläppen av koldioxid och samtidigt hitta en återvinningsprocess för ett material som vanligtvis anses oåtervinningsbart. Detta examensarbete gör just detta. Hittar den bästa processen för att producera ett cementlikt material från kasserad glasull

Materialitet kallas geopolymerer. Geopolymerer ar vanligtvis en blandning av lera med ett högt kisel innehåll och en basisk vattenlösning. I detta projekt så har istället pulvret av lera blandats med ett basiskt pulver, sedan har vatten tillsats till denna pulverblandning. Det har forskats på detta material i cirka 90 år men historien om geopolymer sträcker sig ända till det gamla Egypten. Det finns teorier om att stenaren som utgör pyramiderna inte blev släpade dit utan blev gjutna på plats. Det skulle göra att de kan bäras upp i små bitar viket kräver minder arbetskraft än att släpa hela stenblock.

Geopolymerisation sker på ytan av de material som används. De skapar sedan långa kedjor av kisel och aluminium som blir starka genom att interagera med varandra och bilda nätverk.

Produktionen av geopolymerer är beroende av fyra huvudkomponenter i processen. Först, så är det härdningstemperatur och härdningstid. Hitta rätt temperatur där materialet blir som starkast vid olika temperaturer är mycket viktigt. Sen så är vattnen mängden viktig, det är viktigt att inte tillsätta för mycket vatten då det påverkar styrkan negativt. Sist så är mängden bas viktig. Beroende på hur mycket man tillsätter så kan det skapas olika mycket polymer mellan de olika fibrerna och partiklarna.

Från detta projekt är det visat att för att få ett material som kan mätas med cement så måste minst 13% basiskt pulver användas. Användandet av vatten borde hållas så lågt som möjligt. Dock så måste man se till att blandningen innan gjutning lätt kan formas. För när för lite vatten används så blir geopolymeren för tjockflytande och kan inte fylla alla hörn av en form. Att använda 60°C funkar bäst om produkten härdas i 24h. Om i stället härdningen bara pågår i 4h så borde 80°C användas. Detta för att 80°C ökar reaktionshastigheten men torkar samtidigt ut provet vilket leder till låg hållfasthet. Vid 4h så hinner provet inte torka men reaktionen snabbas på.

Popular scientific summary

What if we could reduce the release of carbon dioxide and at the same time find a recycling process for a material that usually is deemed unrecyclable. This master thesis aims to do just that. Find the best way to produce a cementitious material from waste glass wool.

This material is called geopolymers. Geopolymers are usually made by mixing clays with a high silica content with an alkali solution. In this project, an alkali powder was instead combined with the clay powder and then ordinary water was added. This material has been researched for about 90 years however the history of geopolymers stretches back to ancient Egypt. Where theories suggest that geopolymerization was used to cast the stones that the pyramids are made of. The material could then be carried in smaller pieces and therefore require less manpower than moving whole rocks.

The geopolymer reaction takes place on the surface of rock or clay-based materials. The geopolymer forms long chains of silicon and aluminium that gets its strength from forming networks of the long chains.

The process of making geopolymers from waste glass wool is relying on four main components. First, it is the curing temperature and the curing time. Finding the temperature that produces the strongest material for different curing times is crucial. Then there is the important parameter of the water to binder ratio. It is important not to add too much water cause if you do the structure becomes fragile and cannot carry a lot of weight. The last parameter important for strength is the amount of alkali. The more alkali that is used the stronger the material since more polymer can form between the fibres of glass wool.

From this project, it was found that at least 13% of alkali powder was needed to get a material that could compete with existing concrete however more than 21% of alkali powder did not increase the compressive strength. The use of water should be kept to a minimum when preparing the paste. It is however important to have a paste you can work with so increasing the water amount just a little bit might reduce the strength but increase the usability of the product. Using a temperature of 60°C works best if the product is cured for 24h, but if the product is cured only for 4h to speed up production a temperature of 80°C is better. The difference comes from that the 24h curing at 80°C dries the sample too much but when cured for only 4h one can take advantage of the increased reaction rate from the increased temperature without suffering from evaporation.

Abbreviations

AAM	Alkali Activated material
BP	Best Paste
CS	Compressive strength
DTA	Differential thermogravimetric analysis
FA	Fly Ash
GP	Geopolymer
GW	Glass Wool
MK	Meta Kaolin
OPC	Ordinary Portland Cement
RK	Reaction kinetics
Ref	Reference sample
SM	Standard Mix
Sialate	silicon-oxo-aluminate of Na, K, Ca, Li
SoSi	Sodium Silicate
TGA	Thermogravimetric analysis
WTBR	Water To Binder Ratio
XRD	X-ray Diffraction

Table of contents

1 Introduction

Cement is the most common building material in the world. The production of cement was in 2018 half a tonne per person and year globally. The issue with the large cement production is the CO_2 release (Andrew, 2018). The most common cement is the ordinary Portland cement (OPC) and through the production of structures using OPC the emission of CO_2 is 0.8 tonnes per tonne OPC produced (Zhijun He, 2019). In recent years the energy efficiency in production has been improved to lower the emissions. However, the calcination process needed to reduce $CaCO_3$ into CaO releases CO_2. The calcination is responsible for 50-60% of the total emission for OPC production. This part of the emissions can not be lowered. Therefore the search for a cementitious material with a lower CO_2 footprint is vital for the continuate use of cementitious materials in the construction sector (Andrew, 2018).

One promising alternative to OPC is geopolymers (GP). These materials are inorganic amorphous polymeric structures comprised of silicon and aluminium. GP can be produced at low temperatures and some raw materials do not need to be calcinated (Abdullah et al., 2018). Geopolymer is a term coined by the French scientist Joseph Davidovits in 1976(Davidovits, 2020). The search for a quick solidifying clay-based binder started in the early 1930s with the Belgian scientist Arthur Purdon. He started to experiment with alkali-activated clays. From 1950 to 1970 much work was done in the USSR, mostly by Victor Glukhovsky. He called his binders “soil silicate cements”. Most of these early silicate-based binders were, however, never truly polymers but instead hydrates just like OPC (Davidovits, 2020). Nowadays the GP produced are true inorganic polymers.

These finding in the 20th century is a rediscovery of building technics long-forgotten according to Davitdovitz. He claims to have strong indications that much of the stone goods from ancient Egypt were not carved from existing rock, but instead, cast into shapes. This applies to most Egyptian construction marvels from vases to larger houses Davidovitz argues that through the use of mineral binders the Egyptians were able to cast the great pyramids on site. This means that the stones were transported not as big blocks of stone but as small portions of clay.

There are three main raw materials used for GP production, metakaolin (MK), fly ash (FA) and blast furnace slag (slag)(Davidovits, 2020; E. Petrakis, 2019; Hardjito et al., 2005). Metakaolin is a calcinated form of the natural occurring kaolin clay (Davidovits, 2020). Fly ash is the residue deposit after burning material, usually coal in thermal power plants (Hardjito et al., 2005). Slag is the residue from iron ore purification (E. Petrakis, 2019). Both slag and FA are being phased out as the industries are switching to a more environmentally friendly manufacturing process and the calcination of kaolin suffers from the same problems as OPC. This means that the need to find a material that has a low environmental impact and is readily available is of importance.

It has been shown that glass wool (GW) as a raw material for geopolymerization has potential. GW is one of the most used isolation materials in the world. It is used for thermal isolation and for sound isolation. When GW is discarded both in the manufacturing process and after serving its purpose as isolation it usually ends up a landfill. Today there is no large-scale process to recycle the GW. Therefore the use of GW as a raw material for GP could be the way to advance (Yliniemi et al., 2016). GW has shown to be comparable to OPC in one of the most important tests for usability, the compressive strength test. The compressive strength (CS) of GW has been measured to 48MPa (Yliniemi et al., 2016) which would correspond to a mid-range of compressive strength for an OPC (NevadaReadyMix, 2022). Most commercially available GW is covered with an organic binder, so the fibres adhere to each other. This layer of organic matter has been a concern in the development of the technique. There has been a study on the influence of the organic binder, and it concluded that the compressive strength of the GP is

lowered but that the material still undergoes geopolymerization. It has also been confirmed that the addition of organic binders reduces the water resistance for GP(Lemougna et al., 2021).

When producing GP, the usual method is the so called “two-part” method. This mean that the GP consists of a dry powder of binder and a liquid solution of water and alkali. This alkali solution has a high alkalinity and is viscous. This entails certain problems and safety issues in production. To combat these issues an alternative method has been developed. This is the “one-part method. In this method the dry powder consists of both the binder and the alkali in powdered form, to this water is then added just like OPC (Luukkonen et al., 2018). This strategy is dependent on a quick dissolution of the alkali, that otherwise is prepared days before. A study on different alkali sources for one-part geopolymerization concluded that the best alkali to use is sodium metasilicate penta hydrate.

1.1 Aim

This master thesis aims to find the best parameters for the geopolymerization of glass wool with additions of metakaolin. The parameters that will be evaluated are, curing temperature and time, water to binder ratio and amount of alkali used. The addition of slag will also be investigated. To determine the best combination of these parameters the compressive strength will be measured and used to evaluate. To aid the compressive strength and to evaluate the similarities and differences between different samples, XRD, TGA, microscopy and reaction kinetics will be used.

2 Background

2.1 Silicates

Geopolymers are silica-based amorphous structures. Silicates are the most common minerals and constitute approximately 90% of the earth's crust. The fundamental unit in silicate containing structures is the silicon-oxygen tetrahedron $(SiO_4)^{4-}$ the structure can be seen in *Figure 2.1* and is a cationic silicon ion Si^{+4} surrounded by four oxygen atoms forming the characteristic tetrahedron

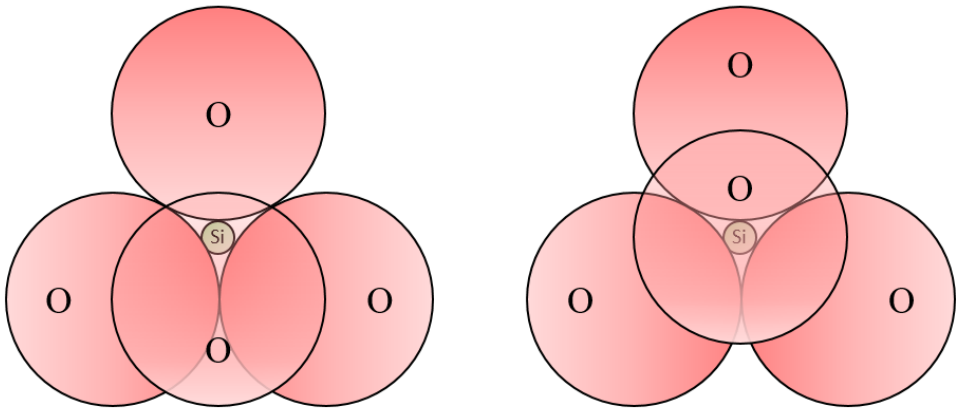

Figure 2.1 The silicon oxide tetrahedron SiO_4. To the left from the side and to the right from the top. Illustrating the positions of the oxygen atoms around the silicon.

The tetrahedrons are kept together by bonds consisting of approximately 50% ionic bond characteristics and 50% covalent bond characteristics. The Silicon ions positive charges are countered by the four oxygens, while the oxygens only constitute half of the bonding capacity to the tetrahedron. This is to be able to form a similar bond to another tetrahedron centred around another silicon ion. These silicate tetrahedrons can be organized in a multitude of ways to form different structures all comprised of silicate. The simplest form is independent tetrahedrons called orthosilicates SiO_4. Then there are double tetrahedrons connected at one point to form Si_2O_7 sorosilicates. Then the tetrahedrons can be connected into ring formations of different sizes from Si_3 to Si_6 rings, these are called cyclosilicates. Furthermore, even more, complex structures can be formed from the original structure. Both one-dimensional links and two-dimensional sheets can be formed. This sheet has a Si:O ratio of 2:5 coming from that three out of the four oxygens are shared with other tetrahedrons. The most complex structure of silicates is the three-dimensional structure. These are however the most common structures. The crust of the earth is composed of 75% three-dimensional silica structures. These are ordinary silicates with the atomic ratio

of 1:2 of silica to oxygen. In *Figure 2.2* from the encyclopaedia Britannica, all the structures described are visualized.

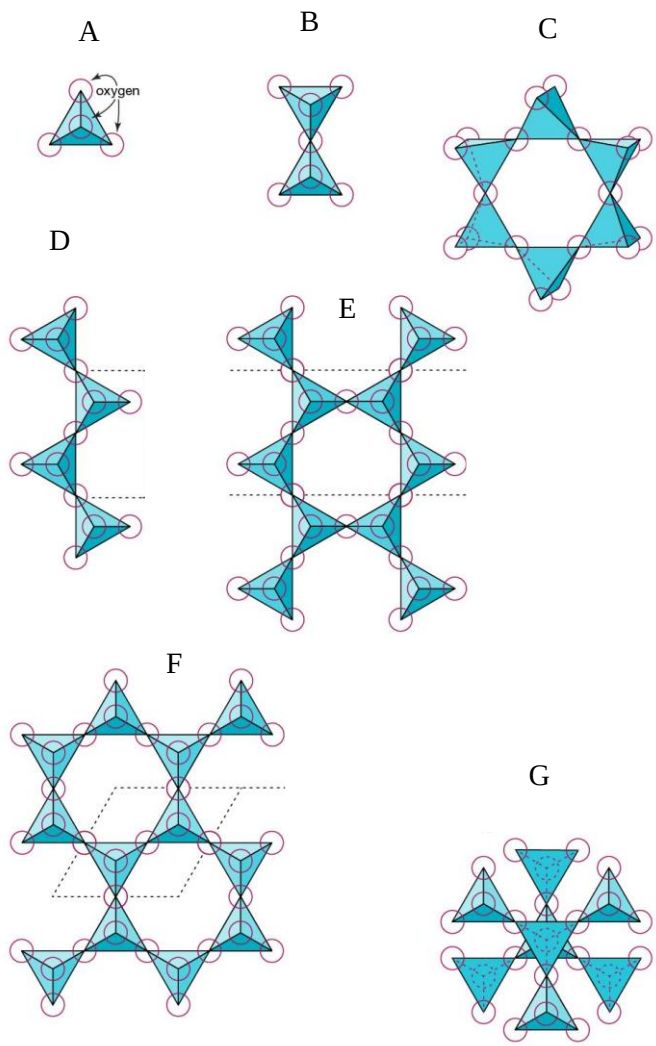

Figure 2.2: Conformations of silica tetrahedrons into more complex structures. A) simple tetrahedron, B) double tetrahedron sorosilicates, C) ring forming silicates cyclosilicates, D, E) are both Inosilicates single and double-chained silicates respectively, F) is the sheets of silicates while G is the 3-dimensional structure of silicates ("Various structural linkage schemes in silicates.," 2022)

2.2 What is a geopolymer?

Geopolymers are amorphous inorganic polymer structures. These structures are normally created at low temperatures compared to ordinary ceramics. Geo-polymers are produced below 100 °C generally. These networks are linked by covalent bonds. Geopolymer exhibits an amorphous structure below 500°C (Davidovits, 2020).

In the early days of geopolymers, there was a debate about whether the bonds in geo-polymers were covalent or ionic. The matter was solved by comparing the bond length of what a covalent bond was and what the ionic bond should be. By using this method, the matter was settled that the bonds in the geo-polymers were covalent (Davidovits, 2020).

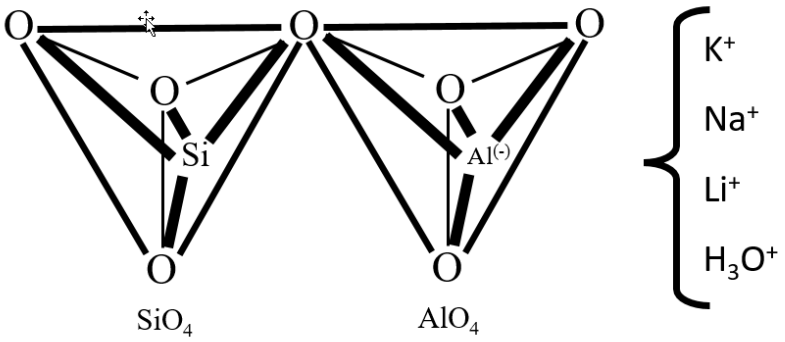

Figure 2.3 The tetrahedral configuration of silicon and Aluminum in a geopolymer structure. Due to the charge of the aluminum atom in the tetrahedron a stabilizing cation is needed. The most common are compiled to the right

2.2.1 Geopolymer nomenclature

To be able to communicate the findings done in the field of geopolymers some terminology has been decided. This has been done mostly by the Geopolymer Institute in Saint-Quentin, France headed by Joseph Davidovits (Davidovits, 2020). The use of the term sialate is common in geopolymer science. This term is an abbreviation for siloxonate which is the silicon-oxygen tetrahedron. A lot of the terminology comes from the field of organic polymers (OP). The terms for macromolecules and oligomeric molecules link over from carbon-based molecules to the silicate-based molecules of GP. There are as in OP oligomers. There are no monomers in GP but the oligomer has replaced the monomer as the smallest constitute in the molecule. The silicon or aluminium tetrahedron could be considered as the monomer. The ratio between them is the dominant difference between different oligomers so use of this monomer would be insufficient (Davidovits, 2020).

The reaction polycondensation that is a common reaction in OP is the main way of producing GP. Instead of forming water as OP, the condensate in GP is MOH where M can be any of (Na^+, K^+ and Ca^+) depending on which one was used as the alkali source (Davidovits, 2020). The different ratios of Si/Al are named as can be seen in *Figure 2.4.*

A

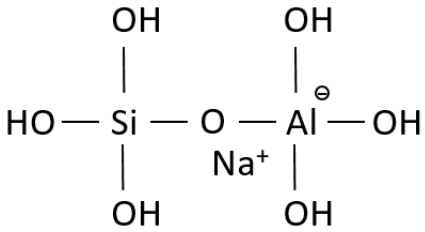

B

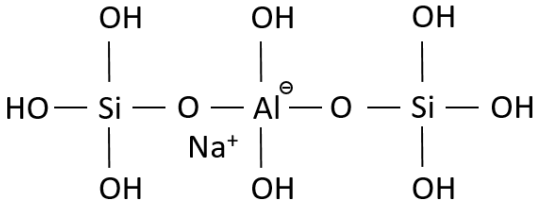

C

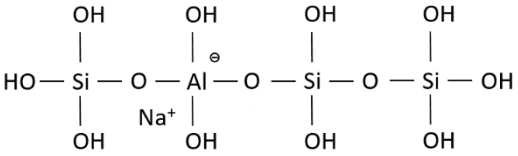

D

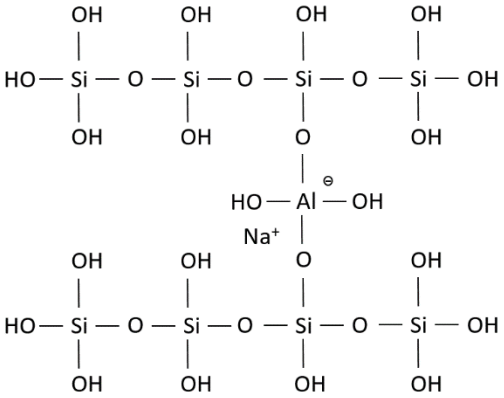

Figure 2.4 An illustration of the different oligomers of sialate based geopolymer building blocks. A: sialate Si:Al=1, B: sialate-siloxo Si:Al=2, C:sialate disiloxo Si:Al=3 and D: sialate link Si:Al>3.

The oligomers are named after the ratio this is further described in *Table 2.1* which contains the oligomer and the name of the polymer formed via polymerisation.

Table 2.1 The names of the four oligomers in geopolymerization together with the ratios of the names and the polymeric name after polymerization

Si/Al ratio	Oligomer name	Polymer name
1	Sialate	poly(sialate)
2	Sialate siloxo	poly(sialate-siloxo)
3	Sialate disiloxo	Poly(silate-disiloxo)
> 3	Sialate link	poly(sialate-multisiloxo)

In all oligomers, the ratio is built into the structure of the oligomer except for the sialate link where the oligomer consists of two poly(siloxonate), poly(silanol) or poly(sialate) with a -Si-O-Al-O-Si- bridge between them thereby the ratio of Si: Al can become high depending on the length of the silicon chain. (Davidovits, 2020)

2.2.2 Production

2.2.2.1 Production materials

This report is about the possibilities of producing high-quality geopolymer from glass wool. Previously, a lot of focus has been on different kinds of ashes. Fly Ash (FA) is a common component in GP. Fly ash is a rest product from the combustion of coal in thermal power plants. The FA is a fine powder separated from the flue gas via a particle separation system on the exhaust. FA is found in abundance around the world and creates storage issues (Hardjito et al., 2005). The use of rice husk ash can be utilized in some areas of the world (Kühne, 2016). The use of FA from thermal power plants powered by household waste is not recommended due to the difficulties of ensuring the absence of heavy metals (Hyunjung Kim, 2012). Other materials such as slag and metakaolin will be discussed more thoroughly later in the report.

2.2.2.2 Production routes

Geopolymers can be produced using one of two main production paths. These are Acidination and alkalination. Using Acid, like phosphoric acid gives different poly silicates such as poly(phosphor-silioxo) and poly(alumino-phosphor-siloxo) compared to alkali-activated such as Na, K and Ca-based hydroxides. These give the poly(silicates) and poly(siloxo). The most common reaction is the alkalinization path. To further divide the reaction paths of geopolymers can be divided into one-part and two-part polymerization. Two-part polymerization is the most common. The difference between them is how the alkali or acid is added. In two-part, the activation substance is added in a premixed solution, while in one-part the activation substance is added in a dry powder form mixed with the other binder and filler material. Then water is then added to the dry mix. This resembles the way OPC is used today. The reason why one-part is being studied is to minimize the risk of transporting and handling alkaline and acidic solutions and instead use powder form and adding water(Davidovits, 2020).

2.2.3 Advantages over Ordinary Portland Cement (OPC)

The advantage of using geopolymer instead of OPC is primarily a significantly lower CO_2 emission. This comes mostly from that the production method of OPC emits large quantities of CO_2. On average one ton of OPC emits 0.78 tons of CO2, most of which comes from the calcination process. The industry for OPC production is responsible for 5-7% of the world's total emission of CO_2 (Zhijun He, 2019). These emissions are not present at the same scale when producing the starting material for GP. However, the use of some raw materials should be avoided to reduce the CO_2 emissions for GP, such as FA and slag. In this project large part of the starting material comes from waste streams. This means that instead of needing energy to properly dispose of the material this energy can be used to cultivate the material into a good starting material for geopolymerization.

2.2.4 Difference between geopolymer and Alkali Activated Material (AAM)

Two different material structures that often get confused are alkali-activated materials (AAM) and GP. These terms are often used as interchangeable, and many scientists mix them both by mistake and ignorance. The fact is that there is a significant difference between these two materials. This difference will be explained in this section.

The most important difference between AAM and GP is the structural system upon which the material is based on. GP are as the name suggests a polymeric structure with a structured network of O-Si-O-Al-O bonds to form an amorphous polymeric structure. AAM has no long chains of tetrahedron formations. They are a precipitate of the minerals in the raw materials that have been dissolved in the high alkalinity of the activation solution. These precipitates are hydrates with water in the structure of the material. This means that the structural foundations of AAMs and GPs are different (Shoaei et al., 2022).

The water included in the structure gives AAMs better protection from water than GPs. The hydrates in AAM are mostly consisting of two different hydrate gels. Ether the calcium-rich C-A-S-H (calcium

silicate hydrate with aluminium substituted in some silicon sites) and N-A-S-H (sodium aluminium silicate hydrate). The presence of these gels is governed by the amount of calcium and sodium present in the sample.

The geopolymer institute tries to keep the AAM and GP separate by using different names on reaction steps in the process. The initiation of the polymerization is called alkalization compared to the alkali activation for AAM. This is due to that in GP the reactants are already reactive enough to undergo polymerization. Therefore, no activation is needed for GP. For AAM, the same reactants are used but the alkalinity of the alkali activator is much greater than for GP. This leads to fully dissolved precursors to later reform into the AAM hydrate (Davidovits, 2020). AAM commonly incorporates the use of NaOH as an alkali activator. By using a mix of NaOH, SiO_2 and Na_2O the alkalinity of the solution is increased drastically resulting in a solution able to dissolve the raw materials (Das & Shrivastava, 2021; E. Petrakis, 2019; Hyunjung Kim, 2012).

An alternative and seemingly simpler way to distinguish GP from AAM and other cementitious materials is the CaO content. To be called a GP the CaO content needs to be lower than 10% (Shoaei et al., 2022).

3 Theory

3.1 Glass wool

Glass wool is produced from sand soda ash and recycled glass. The ratios of the components are changed to get a good quality of the fibres. The Mixture of raw material is fed into a furnace where the temperature exceeds 1400°C to melt the material. When all material is liquid, the liquid glass is transported to a fiberizing machine. The machine forces the glass through small holes of 1 mm using centrifugal force. the rapid movement of the machine results in a thin fibre that solidifies and cools. These fibres are then sprayed with a binder to get them to adhere to each other. The fibres are then compressed and layered to form long mats that can be cut in various sizes (ISOVER, 2022).

The chemical composition of the Glass Wool can be seen in *Table 2.1*.

Table 3.1 the chemical composition of GW for 11 compounds together with LOI at 525C (Loss On Ignition) from(Lemougna et al., 2021)

	SiO_2	Al_2O_3	Fe_2O_3	CaO	MgO	Na_2O	K_2O	TiO_2	P_2O_5	SO_3	Cl	LOI 525 °C
GW	63.8	1.6	0.5	8.4	1.8	16.9	0.5	0.1	0.2	0.7	0.1	7.4

The most common binders are a sugar-based binder and a phenolic binder. These resins make up around 5 to 10% of the weight of the final glass wool. This can be seen in the LOI of GW.

As mentioned before most of the GW is today sent to landfills when they have served their purpose in the construction industry. To use GW as a building block for other silica-based materials could solve this recycling problem. GW has the potential to be used as a geopolymer precursor. The fibres have a chemical composition that works with the GP reaction e.g. have a high Si content and have and have an amorphous structure (Yliniemi et al., 2016).

3.2 Ground granulated blast furnace slag

GGBFS is a residual product of the iron enrichment process. When producing iron from iron ore. The ore is mixed with coke and limestone. This mixture is then melted in a blast furnace. The iron and slag are separated in their molten form at 1500°C. The production of 1 ton of iron results in the production of 200-400kg of slag depending on ore and production parameters (Yuksel, 2018). GGBFS has been used as an additive to OPC for more than 80 years.

In recent years the use of GGBFS in geopolymerization has been studied more. Experiments of mixtures of FA and GGBFS has been done (Saludung et al., 2018). When GGBFS was added to FA in a ratio of 30:70 a maximum was found compared to other ratios. (Kushal Ghosh, 2018). There have also been reports of the highest CS the more GGBFS added to the mixture. The maximum was measured for a GP composed of solely GGBFS (Luga & Atis, 2016) (Hyunjung Kim, 2012).

A reason why some reports claim an increasing CS with the GGBFS content while others claim a maximum can be reached when a mixture is used is the mixing and curing method used. For the samples that exhibited a maximum CS for a 30:70 GGBFS/FA ratio the curing was done for 72h at 100°C (Kushal Ghosh, 2018). While the samples showing that the sole use of BBGFS reaches the highest CS values were cured at ambient temperature. The same samples exhibited a peak value for a ratio of GGBFS/FA separated from zero FA when cured at elevated temperature (Hyunjung Kim, 2012)

3.3 Water to binder ratio

The water content of a geopolymer should be kept to a minimum. This is because the water is not incorporated into the structure like for example in OPC. The water only acts as a transportation path for the ions needed to stabilize the tetrahedral structure of AlO_4 (Duxson et al., 2005).

The water to binder ratio (WTBR) has a large influence on certain parameters for both the processability and durability of geopolymers. The amount of water is closely linked to the flowability of the cementitious paste. Experiments performed with WTBR of 0.16, 0.2, 0.25, 0.30, 0.35 and 0.4 gave the result that the lowest ratio had no flowability at all. The paste was hard and proved too hard to mix or handle no further tests due to the firmness of the paste. For the other ratios testing the flowability of the pastes using a series of tests, the conclusion was that there is a linear relationship between the WTBR and the flowability. It was also found that contrary to low WTBR not being processable, WTBR above 0.35 phase-separated which creates problems when pouring and moulding GP (Patankar et al., 2013).

The WTBR also affects the CS of the geopolymer. A low WTBR results in lower CS due to the lower reaction rate in the dryer samples. The opposite problem arises for samples with high WTBR, the higher ratio leads to a sample that is still wet after the curing process. This excess moisture affects the CS negative (Patankar et al., 2013). A suitable range for geopolymer production is between 0.25-0.35. In this range, the processibility is sufficient enough and the CS is the highest in this range (Patankar et al., 2013).

3.4 Temperature

3.4.1 Curing temperature

The temperature at which the samples are cured has a significant impact on the mechanical strength of the sample. Curing at ambient or close to ambient temperatures results in low CS for early testing compared to 60°C and 80°C. This trend, however, cannot be found after 28 days of ambient curing after the initial mould curing. This disappearance of the CS gap between ambient curing and elevated curing is a result of the lower degree of polymerization for low-temperature curing. Since the gap closes with time the polymerization continues during the storage phase (Rashidian-Dezfouli et al., 2018). The CS is at its highest for curing temperatures around 60°C compared to 80°C or higher. The reason that a higher curing temperature does not increase the CS is the evaporation of water. At higher temperatures the water evaporates before the network is fully formed and therefore the CS is significantly lower at temperatures approaching 100°C (Mo et al., 2014).

3.4.2 Heat release

The exothermic behaviour of geopolymer has been documented. This has led to the standardization of a measuring method to determine the reactivity of geopolymer components based on temperature increase. The method consists of two samples equal in weight and consistency placed in an oven for curing. One sample contains an alkali solution the other only water. The temperature difference is measured with ordinary thermometers and can then be compared to one other. When only metakaolin and a sodium-based alkali solution are used, the peak temperature is reached after 35 minutes. This is a few minutes slower than for and potassium-based alkali solution. When performed at an oven temperature of 80°C the sodium and potassium reached an increased temperature of 29°C and 23°C respectively over the oven temperature. This demonstrates that the geopolymer reaction is exothermic and that this rather simple setup can be used to monitor the geopolymerization (Davidovits, 2020).

3.5 Silicon, aluminium ratio

Experiments on metakaolin have shown, that the optimum ratio of Si/Al is found to be around 2 (Duxson et al., 2005). By mixing different amounts of an alkali solution (SiO_2 and Na_2O) the ratio can be changed

from a metakaolin ratio of 2.3 to ratios from 1.15 to 2.15. for these mixtures, the optimum is 1.9 (Duxson et al., 2007) (Davidovits, 2020).

However, these results are being questioned both for metakaolin and for other types of precursors with different compositions. There have been findings where both the CS and the flexural strength increased when the Si/Al ratio went from 2-to 4. With the highest Si/Al ratio corresponding to the highest CS (He et al., 2016) when even higher Si/Al ratios are used for geopolymerization of stone and glass wool the result is the same (Yliniemi et al., 2016).

An explanation for this is the stronger bond of the Si-O-Si bond compared to the Si-O-Al bond or the Al-O-Al bond (De Jong & Brown, 1980). This would imply that the strongest oligomer in GP is the sialate link and not the sialate siloxo oligomer proposed by Davidovits and Duxson (Davidovits, 2020; Duxson et al., 2007). An alternate explanation could be the dissociation speeds of Si and Al. If Al dissociates from the GW at a higher rate than Si the real composition of the GP will have a lower Si/Al ratio than the theoretically calculated value from the compositions of the raw material (Yliniemi et al., 2016).

3.6 Calcium amount & Mg amount

The fraction of calcium is sometimes counted as one of the ways to decide if a geopolymer is a geopolymer. Because with a too high calcium content the geopolymer could be defined as an OPC (Shoaei et al., 2022). This range does not however take the reaction mechanism into account since the fraction of CaO does not govern the reaction mechanism per se. The amount of CaO in the geopolymer mixture is affected by the strength of the GP in different stages depending on the fraction (Temuujin et al., 2009).

An increasing amount of both CaO and $Ca(OH)_2$ increases the CS for GP when cured at ambient temperature compared to a lower ratio of the compounds (Temuujin et al., 2009).

The amount of Ca affects the CS different for different curing temperatures and different concentrations. For curing at ambient temperature an increasing amount of both CaO and $Ca(OH)_2$ increases the CS. When adding CaO and $Ca(OH)_2$ the CS increases by 2-3 times respectively when adding 3% of Ca containing compounds (Temuujin et al., 2009).

For curing at an elevated temperature of 70 °C the influence of Ca was reversed. When adding 3% of CaO and $Ca(OH)_2$ the CS dropped by 60% regardless of the added compound. The authors argue that this indicates that there is a different reaction taking place between ambient and elevated curing. The difference between CaO and $Ca(OH)_2$ seems to be that $Ca(OH)_2$ is the better option since it increases the CS for ambient more and lowers it for elevated temperature less (Temuujin et al., 2009).

The higher Ca content of stone wool compared to GW is thought to be the reason for the higher CS at ambient temperature. The calcium and silica form a strong bonding system already at low temperatures. This system will give the opposite effect when cured in elevated temperatures. Then this phase will hinder a more stable geopolymeric phase to form which gives rise to the higher CS of GW for elevated temperatures (Yliniemi et al., 2016).

The main reason to add extra MgO is to reduce the shrinkage of the geopolymer. The reduction in shrinkage is due to the formation of MgO chains in the geopolymer paste (Li et al., 2019).

When adding two different MgO compounds one more reactive than the other the shrinking of the Gp gel could be decreased by 20% by adding 6% of reactive MgO. For lowering the shrinkage long term the use of low reactive MgO is preferred (Li et al., 2019).

The shrinkage is an indication of the CS therefore it is used as a measurement of performance. For early testing (3 and 7 days) the CS increased with increasing MgO content (from 4-12%). This means the more MgO added the higher CS in early testing. For 28-day testing there was a maximum for the CS at 8%, above this, the CS decreased with increasing MgO. This would indicate that excessive use of MgO is not recommended and that the recommended dose is between 4-8% (Li et al., 2019).

3.7 Alkali ratio

Experiments performed with liquid alkali solutions have indicated that an increase in alkali solution results in lower CS (Chi, 2017). The ratios solution /binder were 0.35, 0.5 and 0.65. One reason for the conclusion that lower alkali is better could be the increase in water. Due to the pre-dissolved alkali, the mixture has a fixed content of water. So, when the solution is added to the mixture the amount of water is larger compared to binder powders. It is known that a higher WTBR results in a lower CS (Patankar et al., 2013).

For solid one-part geopolymerization, the alkali/ binder ratio can differ from 6% (Sajjad Yousefi Oderji, 219) to 16% (Shuntian Ouyang, 2020) 11% (Cong Ma, 2018). The lower ratios are due to the absence of water that is present in the two-part GP described above.

Since the alkali is not a part of the reaction mechanism but only stabilises the aluminium oxide tetrahedral structures. The need for alkali cannot be decided with molar ratios since the need is governed by the diffusivity of the paste and the dissolution of the surface material. The diffusivity can be improved by mixing the paste thoroughly before adding water and continuing to mix when water is added.

Then the alkali is evenly distributed in the paste and the need to rely on the diffusivity decreases. The dissolution of the alkali is governed by the amount of water in the paste the temperature of the paste and to some extent the mixing of the paste (Chi, 2017).

3.8 Porosity

Porosity is a parameter that can affect the compressive strength and thereby the overall usability of geopolymer cement. Porosity can come from mainly two sources. First, it’s large pores that come from air trapped in the cement during mixing and moulding. The size of these pours is usually large, especially the ones from moulding where the viscosity of the cement stops the paste to reach all corners. The pours from air trapped from mixing. The air is mixed with the paste and is divided into smaller bubbles. These bubbles can be removed by shaking the moulds before curing to force the cement to settle in the mould and expel excess air. The second way of pore formation is by water evaporation. When curing takes place at elevated temperatures some of the water in the paste will evaporate before the gel has settled into formation, this would create small bubbles of steam inside the matrix. The bubbles would then be encapsulated into the matrix. This would increase the porosity of the sample (E. Petrakis, 2019). An increase in porosity would lead to a lowered mechanical strength. According to (Kubba et al., 2018). This is true for temperatures of 27°C, 60°C and 90°C. The porosity could be changed by the change of alkali and the composition of the binding material.

3.9 Particle size

The particle size of the precursor plays an important role in the geopolymerization process. Since geopolymerization demands material to leave the surface of precursors to take place in the reaction surface area needs to be maximized to maximize the amount of geopolymer gel that can be formed. By reducing the size of the particles, the area increases compared to the volume and mass of the precursor

used. By reducing the particle size from 39.9 μm to 11.9 μm the compressive strength increased by a factor of three. This indicates that a smaller particle size would produce a stronger cement(E. Petrakis, 2019). However, in some cases, a smaller particle size could also have negative effects on the compressive strength of a cement mixture. When comparing particles of sizes >4mm 4-2mm 2-1mm and <1mm Horvat and Ducman found the same trend that the compressive strength increased when decreasing the particle size however they observed a large drop in CS for particles <1mm compared to 2-1mm. The explanation they presented was that during the reaction gases were released and since the particle size was small the geopolymer gel sealed all space between the particles and the gases had nowhere to escape. This in turn led to pours forming and decreasing the CS of the geopolymer (Horvat & Ducman, 2020).

3.10 Compressive testing

A common way to measure the mechanical properties of cementitious material is by doing a compression strength test. The tests are performed at certain intervals that are standard for the cement industry. The times are 3, 7, 14 and 28 days. This form of evaluation of the CS comes from the fact that the hardening process of cement is an ongoing process that takes a long time to develop full strength. the most important test is the 28-day test. This is since most of the strength has been reached at this point(NevadaReadyMix, 2022).

The value of the CS is calculated from the failure load divided by the cross-section area. The failure load is the load the concrete is under when it breaks. This load corresponds to the highest force applied or the peak stress (σ). From this point, the sample quickly loses its CS due to cracks and breakage of the sample. *Equation 3.1* calculates the CS.

$$\sigma = \frac{F}{A_0} \qquad \textit{Equation 3.1}$$

where F is the force applied and A is the cross-section of the sample(Dietmar Gross, 2011). typical values for the CS differ depending on the usage of the concrete. For residential purposes the typical value is around 17MPa for larger constructions may need up to 28MPa and some extreme fixtures with high demands on the mechanical properties may need around 70MPa (NevadaReadyMix, 2022).

The stress of a material is usually depicted as a function of the strain that is applied to the material for a given stress. The strain is a measure of how much the sample has been distorted due to the force applied on the sample. It is described by *Equation 3.2*

$$e = \frac{\Delta l}{L_0} = \frac{l - L_0}{L_0} \qquad \textit{Equation 3.2}$$

The relation described is the engineering strain where *e* is the engineering normal strain, L_0 is the initial length of the sample and *l* is the actual length at every moment in time. The strain is positive if the material is elongated and negative if the material is compressed. These two measurements stress and strain can be used to form a stress-strain curve to describe the mechanical properties of a material. As can be seen in *Figure 3.1* a stress-strain curve can be divided into different parts depending on the material properties that are being exhibited by the material at certain applied stress.

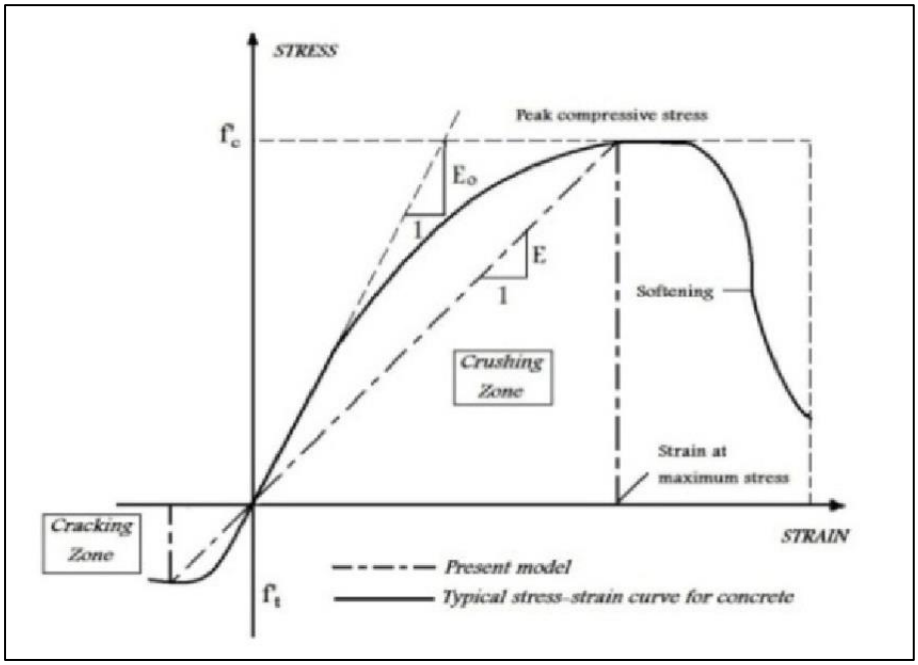

Figure 3.1 Stress-strain curve for a material exhibiting stress and strain through the pashes, young's modulus, yield strength, strain hardening, necking and fracture (Ardebili & Mirzabozorg).

The first part of the graph until the peak compressive stress is the crushing zone and this is often simplified by a linear function as the dashed line in *Figure 3.1*. After the peak compressive strength is reached the stress is lowered for the material with increasing strain this is due to breakage in the material and softening in the strength (Ardebili & Mirzabozorg).

3.11 Thermogravimetric Analysis

Thermogravimetric analysis is a thermal analysis method in which the weight change is measured over time with changing temperature. The weight change can then be presented as a function of time or temperature. This method can be used to obtain information on phase transitions, chemical decomposition, and absorption. The environment of the sample can be set to different atmospheres, oxygen, nitrogen or air. Different temperature programs can be set both where the temperature is increased at a steady pace and where it is fixed for a longer time and then raised to another fixed temperature. This can be altered depending on what type of information is expected from the experiment (J.M.G Cowie, 2007).

From the TGA the evaporation of water will contribute to the largest decrease in weight. For Geopolymers three different types of water can leave the structure.

- Physically bonded water evaporates at 20-100°C
- Chemically bonded water evaporates at 100-300°C

- And hydroxyl groups evaporate above 300°C

Since water is used as a transportation media for the ions in the reaction water is needed in the structure when hardening. But with time the water evaporates out of the structure. Some water however will remain in the geopolymeric-framework, much like water would be trapped in a zeolite framework. The hydroxyl groups are present on the surfaces of the geopolymeric-micelles. These hydroxyl groups can react with each other and form Si-O-Si bonds. This happens at a temperature above 300C. Where the outer -OH groups of the geopolymeric micelles start to react with each other to form liking structures between them. This Is illustrated in *Figure 3*.2 (Davidovits, 2020), (Lemougna et al., 2020).

$$R — OH + OH—R \leftrightarrow R — O — R + H_2O$$

Figure 3.2 Dihydroxylation of OH groups on the surface of geopolymer micelles

TGA measurements have been done for raw GW by scientists from Finland and Belgium. These scientists were looking at the influence of the organic binder used in GW production. They compare samples of GW without an organic binder (OB) to one sample of GW with a sugar-based binder and one with a phenolic binder. The result was that the GW without OB had a weight loss of less than 0.5% when going from 25 to 1000°C. Both of the OB GW had similar TGA:s where the difference is that sugar binder decreases 1% more than the phenolic and reaches a stable weight at 500°C compared to 540 for the phenolic. The decrease for both OB:s starts at 200C. The OB could therefore be decomposing between these temperatures (Lemougna et al., 2021).

The similarities with AAM when preparing GP does so that it is advantageous to compare to publications written about AAM. For AAM prepared from aluminosilicate glass, the TGA has a large decrease in weight between 25-200°C. the first part of this drop is assigned to the loss of added water that has not yet fully dried while the other part 100-200°C is attributed to the water in a C-(N)-A-S-H gel. During these temperatures the main part of the mass loss for AAM takes place. Around 300-350°C, another increase in loss is observed. This loss is connected to the loss of water in the hydrotalcite structure ((Mg6Al2(OH)16CO3.4H2O)). This dehydration is moved along the temperature axis depending on the main precursor for the GP chosen (Mohammad I. M. Alzeer, 2021).

For the SoSi compound with the Na:Si molar ratio of approximately 2:1, the thermal behaviour in TGA shows an initial increase when going from 25°C to 1000C with 5°C/ min in a CO_2 atmosphere. This increase was small and after 130°C the sample started to lose weight. There were two separate losses in weight one between 130°C and 700°C and one from 700°C to 950°C. these phases of weight loss were associated with dehydroxylation and decarbonisation. Since these samples were prepared from silicon oxide (SiO_2) and sodium carbonate (Na_2CO_3), this was then calcinated to get rid of the CO_2 from the structure (Rodríguez & Pfeiffer, 2008).

When analysing the TGA data the 1st derivative of the TGA could be a good tool. This is often referred to as the differential thermogravimetric analysis or (DTA). The DTA gives a clear view of each change in weight of the samples as they appear as peaks in the DTA rather than a decreasing curve (J.M.G Cowie, 2007).

In the differential thermogravimetric analysis (DTA), the melting of crystal structures can be seen as rapid changes in the derivative. This change is in the magnitude of several 1/min in just a few seconds. This sudden alteration is only visible in the DTA. This is according to one source (Rakita et al., 2016).

3.12 X-ray diffraction

The use of X-ray powder diffraction is a powerful tool in material chemistry. It is a rapid analytical method to determine the crystalline structure of a sample.

X-ray powder diffraction XRD can give answers on the average bulk composition since the sample is milled into a fine powder and mixed as a preparation for the XRD. The sample is then placed into the machine that consists of one X-ray source and one detector placed on a circular track that can move around the sample. The X-ray source and detector move in a synchronized way to always have the same angle compared to the vertical of the sample.

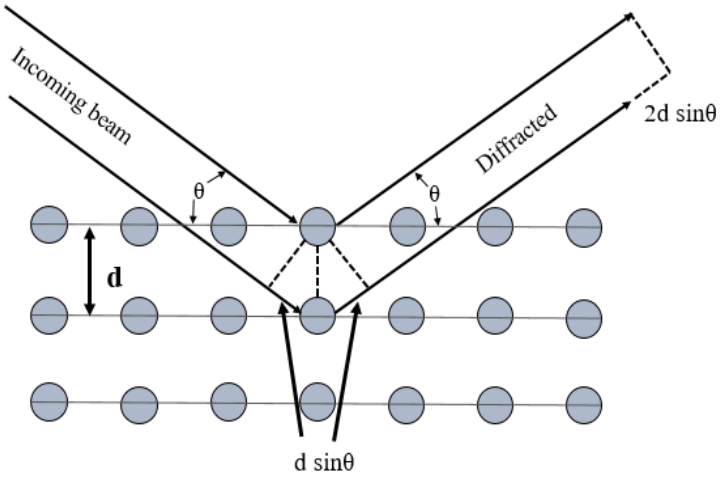

Figure 3.3 the mechanism of X-ray diffraction

The distance between atom layers in a crystal can be calculated using Braggs law *Equation 3.3*

$$\eta\lambda = 2dsin\theta \qquad \textit{Equation 3.3}$$

Where η is any integer, and λ is the wavelength of the beam. This wavelength changes depending on which X-ray source is being used in a certain machine. d is the distance between two crystal planes and θ is the angel between the beam and the crystal plane. When multiplying d with the sine of θ the distance the beam has to travel extra is obtained. This distance is the doubled since the beam travels tis distance both before and after the atom interaction. When this distance corresponds to an integer multiple of the wavelength the detector response is increasing in intensity due to the multiple beams with the same wavelength reaching it. Therefore, from θ knowing the wavelength of the X-ray the distance between atom planes can be calculated. By changing the angle at which the detector a source sits in contrast to each other a spectrum of angles can be analysed. These angles are however not the Theta angle but the 2-Theta angle. This comes from the way that it is possible to measure the angles in the experiment. Since theta is the angle between the beam and the crystal plane, no detection can be done at the angle of the plane. The intensity of the sample is measured on the outgoing diffracted angle which by definition needs to have been diffracted at an angle of 2-theta, one for the incoming beam and one for the diffracted beam (Lesley E. Smart, 2005).

Since different crystals have different d values and different 2-theta angles the information given by an XRD spectrum can show the appearance of different materials in a sample. However, the interference between different crystal structures and the presence of amorphous materials can make the spectrum harder to read than that of a single crystal x-ray diffractogram.

4 Material

4.1 Glass wool

The glass wool used comes from the production at Ecophon and is produced at ISOVER in Billesholm. The wool has been shredded and then ball milled into a powder. This powder contained a varying particle distribution as well as paint residue from the isolation board that had been discarded after painting. To get rid of the larger flakes of paint and some larger fibres the GW was sieved through a series of sieves, the smallest was 500 µm

4.2 Metakaolin

A specific kind of high reactivity metakaolin MK was used. Metakaolin is produced by calcinating kaolin which is a naturally occurring mineral clay. By changing the temperature of the calcination process the metakaolin gets different properties. To reach the high reactivity of metakaolin a temperature between 650-700 °C. Metakaolin is mostly used as an additive to OPC where it increases the workability of the wet paste as well as improves the colouration into a whiter result. The workability improvements lead to a smoother finish.

4.3 Sodium silicate

Sodium silicate referred to as SoSi is a free-flowing soluble sodium disilicate. The composition of SoSi is approximately 27.5% of Na_2O, approximately 56.0% SiO_2, and approximately 16% water calculated from loss on drying. SoSi has good cold-water solubility of 60% dissolved after 1 min for a 1% solution. The pH of a 10% solution is 12. the particle size distribution of the product is less than 5% is larger than 0.5 mm and less than 3% is smaller than 0.063 mm (Woellner, 2015).

4.4 Slag

The slag used in the project comes from SSAB. The slag is ground into a fine powder with a d90 of 10 µm.

5 Method

5.1 Sample preparation

5.1.1 Mixing

The mixing procedure is important to get a homogenous paste to fill the moulds with. Since the objective of the project is to find good characteristics for a one-part geopolymer first all dry components were mixed for 3 min in a food mixer. After that, the water was added, and the mixture was mixed for an additional 10 min. This is to make sure that the paste is well mixed and that the water-soluble SoSi is dissolved. Then the paste was poured in a silicone mould with 9 cubes with 20mm sides. The mould was placed on a shaking table for 3 min to get rid of bubbles in the paste.

The calculations for different percentages and ratios are done by what is mostly done in literature for GP and easy comparison to two-part GP.

$$GW\% = \frac{m_{GW}}{m_{GW} + m_{MK}} \qquad \textit{Equation 5.1}$$

$$MK\% = \frac{m_{MK}}{m_{MK} + m_{GW}} \qquad \textit{Equation 5.2}$$

$$SoSi\% = \frac{m_{SoSi}}{m_{SoSi} + m_{GW} + m_{MK}} \qquad \textit{Equation 5.3}$$

$$WTBR = \frac{m_{water} + 0.16m_{SoSi}}{m_{dry\,mix}} \qquad \textit{Equation 5.4}$$

The binder is referred to as the GW and MK, this gives that the percentage of these are calculated by *Equation 5.1* and *Equation 5.2* respectively. The SoSi percentage is calculated on how much weight the SoSi is of the total dry mix according to *Equation 5.3.* The WTBR is a ratio between the mass of the water and the dry mix and not just the binder calculated from *Equation 5.4.* The WTBR includes the water added and the water from the SoSi which consists of 16% of water.

5.1.2 Standard mix

The method used to investigate parameters affecting the mechanical strength of geopolymers was to compare differences in the parameters to a standard mixture and procedure. This sample called Standard mix (SM), composition and procedure come from the previous testing done at Ecophon as a pre-study to this master thesis. All samples prepared will then be compared to this sample that will be present in all the experimental data from the test, for easy comparison. The percentages in *Table 5.1* are calculated according to *Equation 5.1-5.4.*

Table 5.1 The composition and method of the SM calculated from Equations 5.1-5.4.

	GW %	MK %	SoSi %	Water to binder ratio	Curing time (h)	Curing temp (°C)
SM	80	20	21	0.31	24	60

5.1.3 Best paste

To investigate the best consistency of a geopolymer paste i.e., the most usable paste. An experiment to find this subjective best paste (BP), was constructed. When the paste went to a firm liquid and no longer

retained its form and could self-compact but before the paste got to liquid like state the BP was found. This was done by adding small amounts of water to an existing 0.31 mix. Each addition was evaluated so the procedure took 20 min. which is 3 times the normal mixing time. The result was that the WTBR got to 0.43.

5.2 Curing

5.2.1 Curing method

When the samples were ready to be placed in the oven, the moulds were sealed in a Ziplock bag. This is to prevent the water from evaporating leaving the geopolymer to desiccate before the reaction could take place. The bag was also used when ambient or slightly above ambient temperatures were used to keep the similarities between sample sets. The bag was then placed in an oven (VWR VENTI-Line) for the predetermined time at the selected temperature for each experiment. There were two different curing times used. First, 24h was utilized since this is the standard curing time for geopolymer. Then a shorter curing time of 4h was also investigated to lower production time and energy consumption.

5.3 Analytic methods

5.3.1 Reaction kinetics

To measure the kinetics of the reaction (RK), a setup consisting of thermometers and beakers was used. The thermometers (Testo Saveris 2) measured the temperature every 15 min then the data was wirelessly backed in a cloud service every 15 min, where the data could be collected. The thermometers had a dual probe setup. The data was later processed. The samples are placed in a beaker with a total volume of 200ml. The beaker is filled with 80 ml equal to 5cm in height. Then the thermometer probe is placed into the sample protected by a thermally fused pipette. This is to prevent the material to adhere to the surface of the probe. Tests were made to ensure that the pipette did not inhibit the transfer of heat from the sample to the probe. In connection to this sample, a reference sample was used. This reference consisted of the same parts: probe, beaker, and pipette, but the sample were pure GW mixed with water. Therefore, no reaction took place, but the consistency and amount of water could be controlled and be kept comparable. Then both beakers were placed in an oven to monitor the heat increase both for the sample and the reference.

5.3.2 Compressive strength testing

The CS is the measurement used to give a value to the toughness of the different mixtures and conditions used. The measurements were made on a Tinius Olsen 50ST mechanical testing device can be seen in *Figure 5.1*. The decent speed was of 1mm/min. The compressive strength is measured in MPa which is calculated by the equation from section 3.10. The dimensions of the samples are 20 mm x 20 mm total area of the samples is 400 mm^2 = 0.0004 m^2.

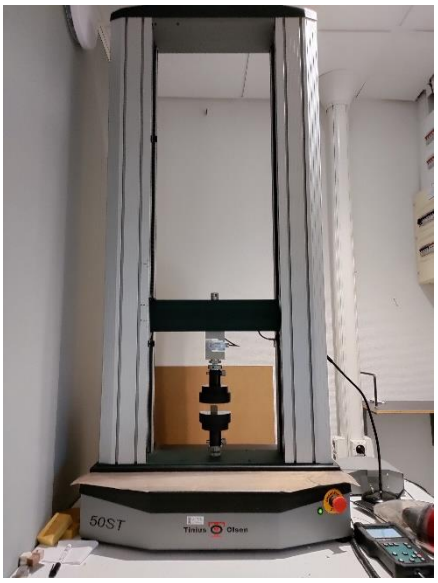

Figure 5.1Picture of the compressive strength apparatus used in the project

For the measurements carried out in this project, the ultimate strength will be used as the measurement for mechanical rigidity. This does not imply that the material will perform at this level all the time. As can be seen in *Figure 3.1* the yield point might be a better measurement since the material has not undergone any plastic deformation at that strain. However, in most measurements performed in other articles, both about OPC and GW the measurement they have used is the ultimate strength also called the Compressive Strength (CS)

5.3.3 TGA

To investigate the thermal stability of Geopolymers TGA was done on the samples. The samples were crushed into a fine powder then between 20 and 40 mg of powder was placed in an aluminium oxide cradle and placed in the autosampler of the TGA. The program parameters set for the TGA was a ramp from 25°C to 800°C with an incline of 10°C/min.

5.3.4 XRD

The XRD was done from 5° to 55° with a copper (Cu) anode emitting X-rays at 1.5406 Å. Three samples were analysed as well as the raw materials for the samples. To get a good result the material should be pulverized to a particle size less than 0.075mm. The was mortared by hand before the samples was processed.

6 Result and discussion

The result of this project is divided into parts of XRD, TGA CS, RK and porosity results. These will be presented and discussed with conclusions drawn between results from different measurement methods. The results that carry the most significance are the CS since this is a common technique used to measure the mechanical properties of cementitious material (NevadaReadyMix, 2022). This means that the results in this section can be compared to other studies done on cementitious materials.

6.1 XRD

XRD was done for all raw materials and three samples with composition and methods seen in *Table 6.1*. The difference between A, B and C, is that B has less SoSi than A and C and that C has the addition of slag compared to sample A and B.

Table 6.1 The composition and method for the three samples analysed by XRD

	GW (%)	MK (%)	Slag (%)	SoSi (%)	Curing
A	80	20	0	43	24h, 60C
B	80	20	0	20	24h, 60C
C	80	10	10	43	24h, 60C

The graphs of A and B in *Figure 6.1* are similar since the composition of them are the same except for the amount of SoSi used (for a more detailed figure comparing A, B and C see *Appendix A*). When comparing C which contains 10% of slag to the other two samples peak 7 is the main difference. This peak can be associated with structures in the raw slag. There are also two peaks 8 and 9 that are missing or not prominent in C. Since everything in A and B also can be found in C this is unexpected.

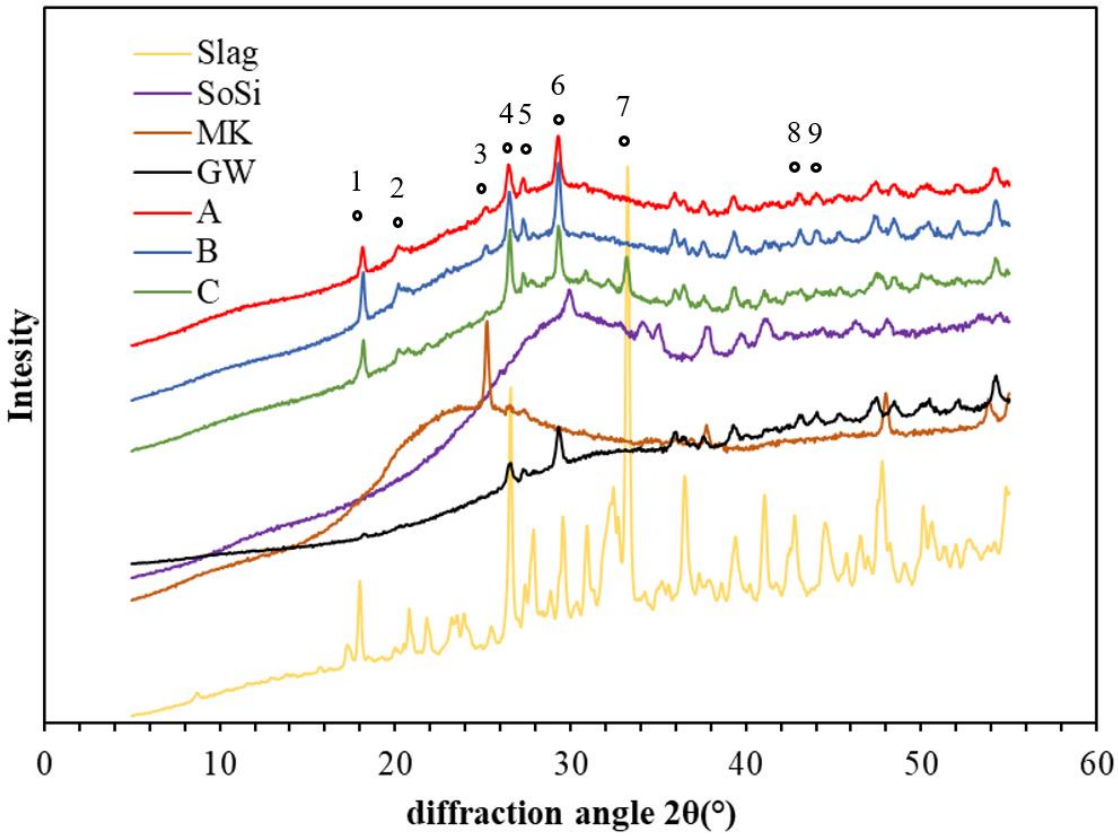

Figure 6.1 The XRD graphs for the three samples A, B and C together with the raw materials GW(Black), MK(Brown), SoSi(Purple), slag(Yellow). The XRD is measured between 5° and 55°.

When comparing the samples to the raw materials the overall trend for the samples is the large amorphous peak (2-theta of 20°-35°) dominating the samples. This peak is located at the same angles as the amorphous peak for SoSi. From TGA the argument is suggested that most of the SoSi has been dissolved since its characteristics are not found in the TGA. So, the fact that all three samples resemble this peak might just be because of the amorphous structure in SoSi and the amorphous structure in the samples have a similar diffractive expression. The increase in intensity is also broad so it could include a multitude of amorphous structures.

Peak 1 is a peak that is faint in GW but is prominent in all samples. This means that this crystal has been formed during the reaction. Peak 2 is only visible in the samples, so it was probably formed during the reaction. Peak 3 is situated for the sample at the same theta value as a large peak in the metakaolin. This indicates that some residual of this crystal is still intact but that most of it have reacted in the reaction. Peaks 4 and 5 can be found in the GW. 4 is also prominent in the slag and might contribute to the slightly higher peak for C compared to A and B (See *Appendix A*). Peak 6 can be found in GW. But the peak from SoSi just beside it is not visible in the samples. Peak 7 and the smaller peaks between 6 and 7 on the C sample all come from the slag since it does not appear in A and B. Peaks 8 and 9 can be seen in sample A and B but is not visible in samples C. these peaks also correlate to a small set of peaks in GW.

The fact that some crystal structures are present both in the raw materials and in the samples concur with the literature since the reaction only takes place on the surface or close to surface. However, there is a lot of peaks that are present in the raw material that has disappeared in the samples of GP. This would indicate that there has been a complete dissolution of the material. This is probably true for SoSi since the goal is to dissolve all of the SoSi but the MK and GW should not all have been dissolved and when

analysing the samples under microscope in *Figure 6.12*. all samples analysed showed intact GW fibres at 115x zoom.

6.2 TGA

Looking at the raw materials in *Figure 6.2a* the metakaolin has no significant decrease in mass for the duration of the experiment. The GW has a small decrease up until 100°C and is then stable until 225°C when a larger decrease in mass is apparent, there is also a rapid drop around 750°C. looking at the derivative in *Figure 6.2b* the different decreases are easier to acknowledge. According to the literature, both the drop at 225°C and 750°C can be attributed to the presence of phenolic binder in the sample(Lemougna et al., 2021). Carboxylation of the phenolic binder is a reasonable explanation for the decrease above 700°C (Rodríguez & Pfeiffer, 2008).

For the SoSi the decrease starts at around 130°C which continues to around 500°C agreeing with the literature (Rodríguez & Pfeiffer, 2008). This decrease of approximately 16% is the water that can be found in the SoSi structure (Woellner, 2015).

a)

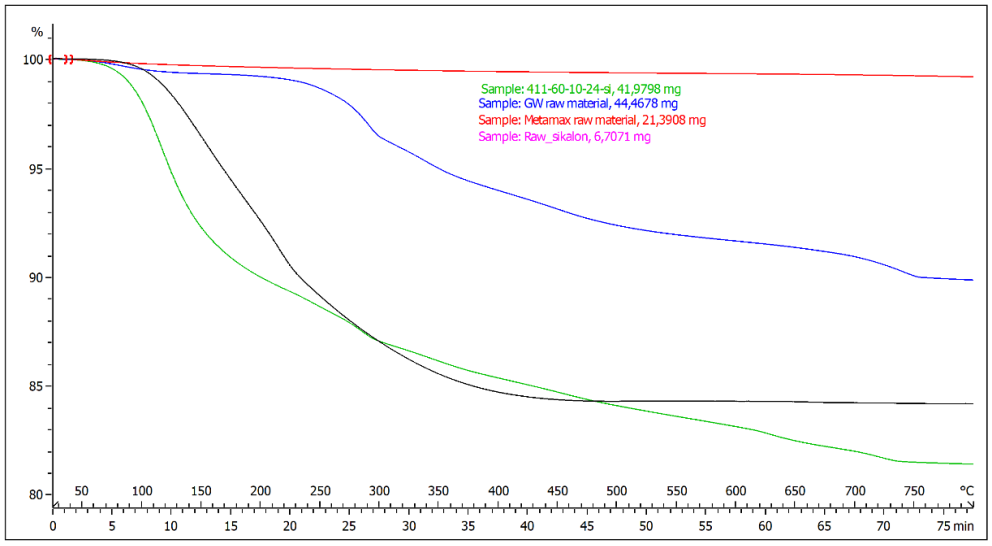

b)

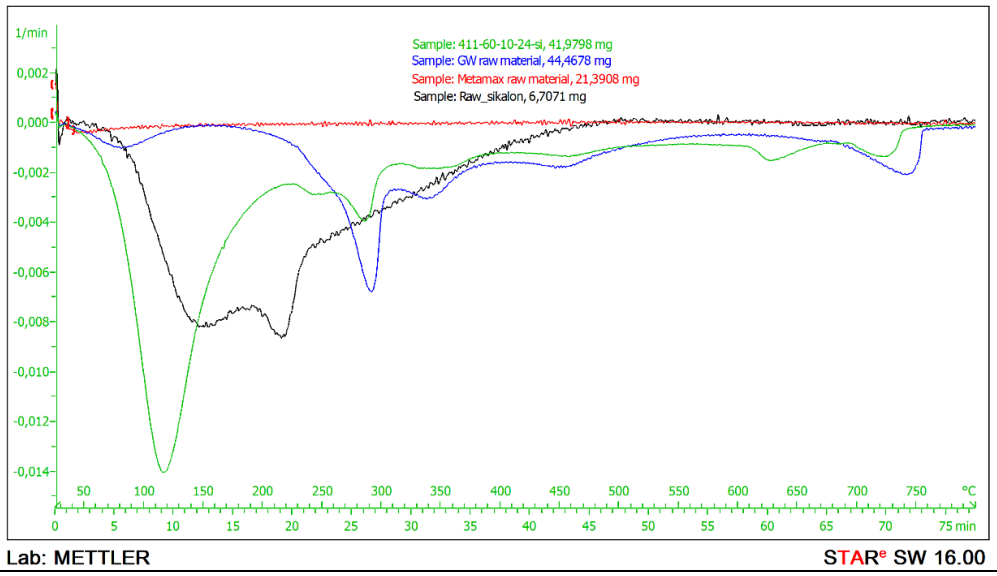

Figure 6.2 a) The TGA of the SM with the raw materials SM (Green), GW (Blue), Metakaolin (Red), SoSi (Black). b) The 1:st derivative of the weight loss from a), SM (green), GW (Blue), Metakaolin (Red), and SoSi (Black).

To analyse the sample SM *Figure 6.2b* is used since the derivative gives a clearer view of the events on the TGA curve. First, there is a large decrease from 25°C to 100°C this is due to residual water in the structure from the preparation of the sample. The water evaporating from the SoSi is not prominent in the sample of GP this indicates that most of the SoSi is dissolved, and the water has been dissolved with the SoSi and joined with the added water. This since the sample decreases in weight change above 120°C while the SoSi raw material keeps evaporating water util 240°C. The next decrease is around 300°C which matches the changes in the phenolic binder from the GW. The same pattern applies to the decrease at 700°C, the binder is decomposed and therefore a decrease is visible there. An interesting change for the SM is the change at 600°C since none of the raw materials exhibits this large of a weight change.

In *Figure 6.3* Samples with different WTBR are presented. In this figure, both the weight loss and the 1st derivative are combined in the same diagram. The large rapid alteration for both the 0.57 and 0.70 is only visible in the DTA. This could be the sign of a crystal phase transition (Rakita et al., 2016). However, the fact that not all samples exhibit this behaviour combined with the XRD results in 6.1, indicates that this might not be the case. These could then be due to artefacts of external influence since no other samples exhibit these fluctuations. The rearranging of a crystal phase should be happening at the same temperature for all samples. If these alterations are neglected the curves are continuous past these points and no changes are apparent at the alteration points.

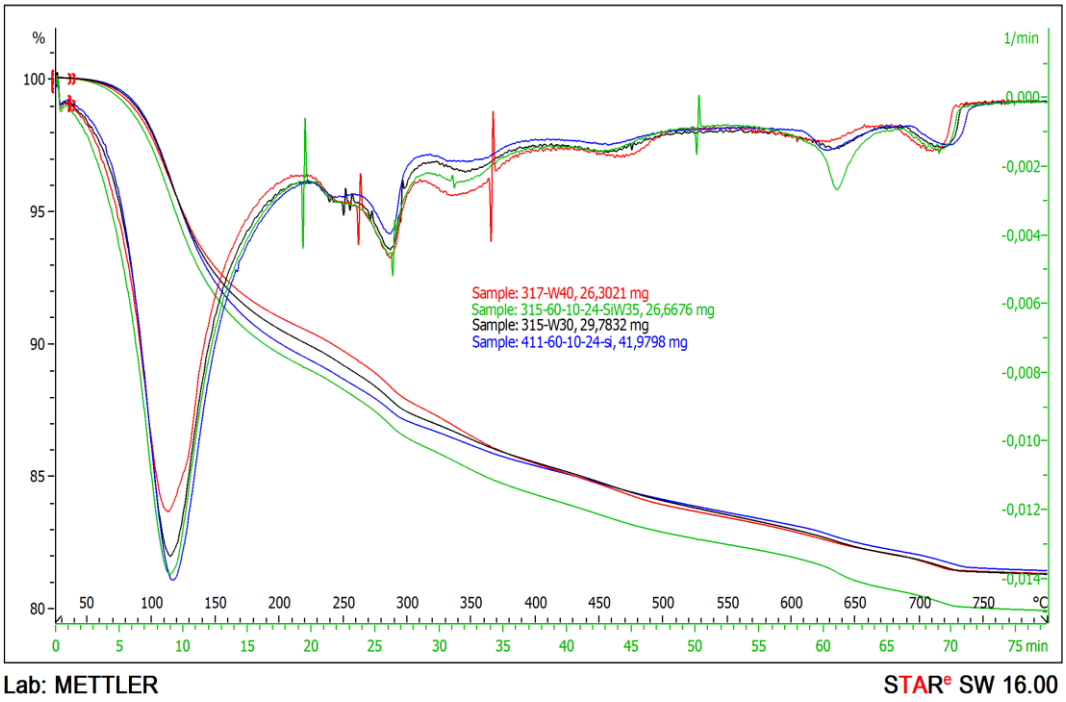

Figure 6.3 The graph of the TGA and the DTA of the WTBR series with the TGA as the decreasing curves and the DTA as the alternating curves. With the graph colors:0.31 (blue), and 0.46(black), 0.57(green) 0.70(red).

When comparing the different graphs, the fact that the curves do not conform to an order of water amount in any way is coherent with the reaction kinetic measurements. Something is happening between 0.57 and 0.7 that has not been explained by these tests. The fact that the sample with the most water i.e., 0.7 is the driest of the samples while the wettest of the samples is the driest mix 0.31 can be explained by *Figure 6.12*. It is visible that 0.7 has a larger number of pores in the structure. This would make the drying process more effective since the water has more pores to escape the sample compared to 0.31.

For the experiment with SoSi amount, the result can be seen in *Figure 6.4*. The samples with 21% (SM) and 26% of SoSi are following each other at almost all temperatures except at 600°C where the sample

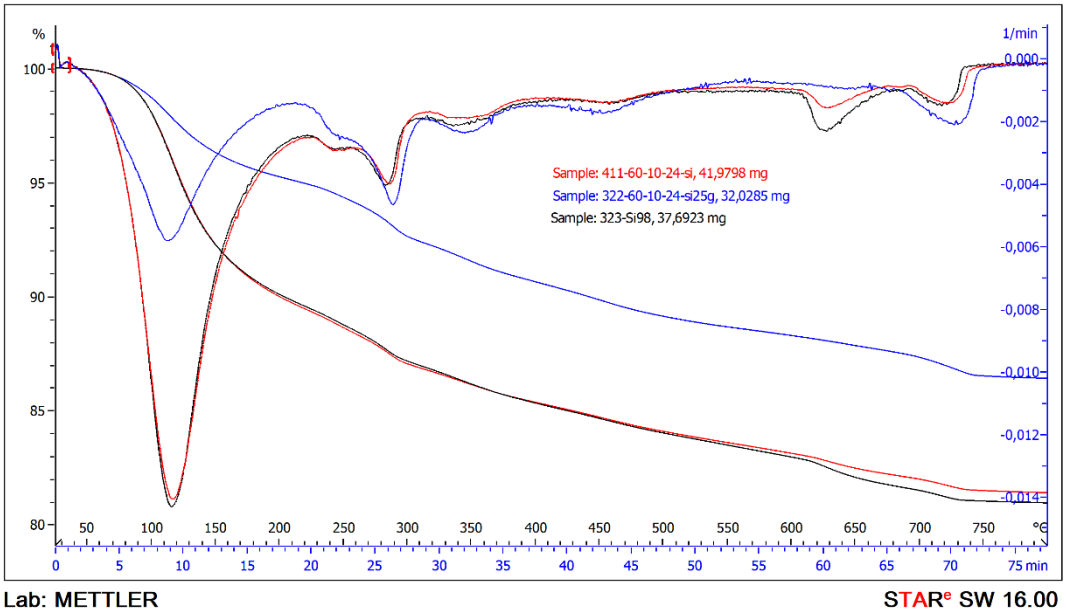

Figure 6.4 The graph of the TGA and the DTA of the SoSi series with the TGA as the decreasing curves and the DTA as the alternating curves 8% (Bule), 21% (red) and 26% (black)

with 26% SoSi decreases a little bit more than the 21% SoSi (SM) sample. The sample with 8% SoSi distinguishes itself a lot from the other two with a drastically lower mass loss. The most significant difference is the water in the sample (up to 100°C) where the sample loses only around 4% of weight compared to the other two loosing 9%. There is also a difference in the TGA between 8% SoSi and the other two at 600°C where the 8% SoSi does not ha a decrease in mass.

The weight change at 600°C is interesting since it is visible in most samples of GP but not in any of the raw materials. The presence of this decrease is not equal for all samples. It is the largest for the sample with an WTBR 0.46 and in 26% of SoSi. In 8% SoSi it is almost non existing. This phenomenon needs further investigation to be determined. A hypothesis is a transition from amorphous to crystalline that happens at 500C according to Davidovits (Davidovits, 2020).If the size of the change could determine the amount of GP the 8% sample would have a significantly lower CS compared to 26% this is true from *Figure 6.7*. At the same time 0.46 WTBR should have a higher CS than 26% SoSi. This is however not the case. Comparing the CS of the samples form *Figure 6.6* and *Figure 6.7* respectively it is seen that 26% SoSi has a CS 2.6 times larger than 0.46 WTBR at 28 days.

6.3 Compressive strength

6.3.1 The Compressive behaviour of Geopolymers

The plastic deformation of the geopolymer is up to 1,5 longer than it is for OPC at similar ultimate stress when compared to values from (Constructor, 2007). The elongated plastic deformation is more prominent when a sample has higher water content and or shorter drying time. The stress-strain curve for SM at 3, 7 and 28 days can be seen in *Appendix C.* Also, the stress-strain curve for four different samples at 3 days test can be seen in *Appendix D.* The elongated plastic deformation of the GP especially at short drying times indicates that the firmness of the paste might be influencing the CS of the dried sample. This would distort the samples showing low CS, this might not be measuring the CS of the GP but instead the CS of the undried paste. The cubes that showed these elongated plastic behaviours would start to flow out on the sides and not crack like OPC and the GP showing the higher CS.

6.3.2 Ultimate stress comparisons

The CS of a material can tell a lot about its structure and other properties. As mentioned before the project has used a standard mix for the preparation of samples this SM is then compared to changed parameters in the mix and method of preparing the sample. This SM is marked with a green square around it as it is present in all graphs of CS.

6.3.2.1 Temperature

Figure 6.5 shows how the CS changes with the curing temperature. The mix of components and mixing method is the same for all samples as is the curing time (24h). The different curing temperatures each have three different measurements 3, 7 and 28-days.

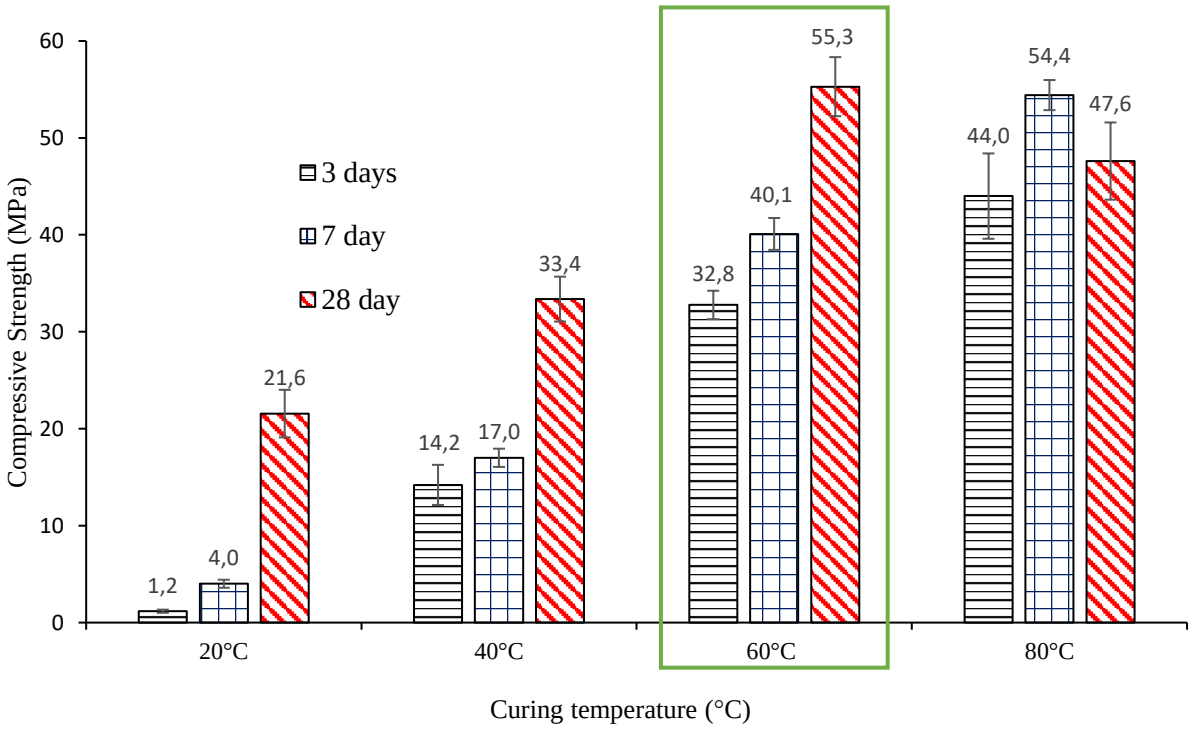

Figure 6.5 Results of CS for the different curing temperatures 20°C, 40°C, 60°C and 80°C. 60°C is the SM this is indicated by the green square. The measurements were done for 3, 7 and 28 days.

It is visible from *Figure 6.5* that ambient or slightly increased temperature gives low CS for 3 and 7 days. For 20°C (ambient) the CS is only 1.2 at 3 days. The sample was also kept in the mould for 24h extra since it could not retain its form well enough to demould after the ordinary 24 h in the mould. This was not enough time since the sample deformed during drying as can be seen in *Appendix E*. However, the Cs increased from 4,01 to 21,56 MPa in 14 days. This indicates that the reaction is ongoing in the material. This trend with increasing CS with time is prominent for all temperatures except 80°C, where the highest CS is measured already at 7 days. The increase in CS with time for samples cured at elevated temperatures indicates that even after curing in the oven the reaction continues not only when temperature conditions are kept constant through curing and drying as for 20°C. For 40°C more than 50% of the total Cs at 28 days comes after the 3day test. The percentage of post curing hardening decreases with temperature increase. The opposite is true for the CS at 3 days, which increases with temperature.

6.3.2.2 Water content

The influence of water amount on the CS was investigated and presented in *Figure 6.6*. The different WTBR are 0.31 0.37, 0.46, 0.57 and 0.7 calculated according to *Equation 5.4*. All samples in this series had the same curing condition of 24h at 60°C, demoulded and dried at ambient temperature and humidity until testing. The highest CS was reached for the sample with the lowest WTBR. Then the samples exhibited a decreasing CS with increasing WTBR. For the WTBR below 0.7 the trend of increasing CS over time is consistent. For WTBR of 0.7, the CS stays the same from 3 days 7 days and 28days. When calculating the CS decrease per increase in WTBR the decrease in CS is the largest between 0.31 and 0.37.

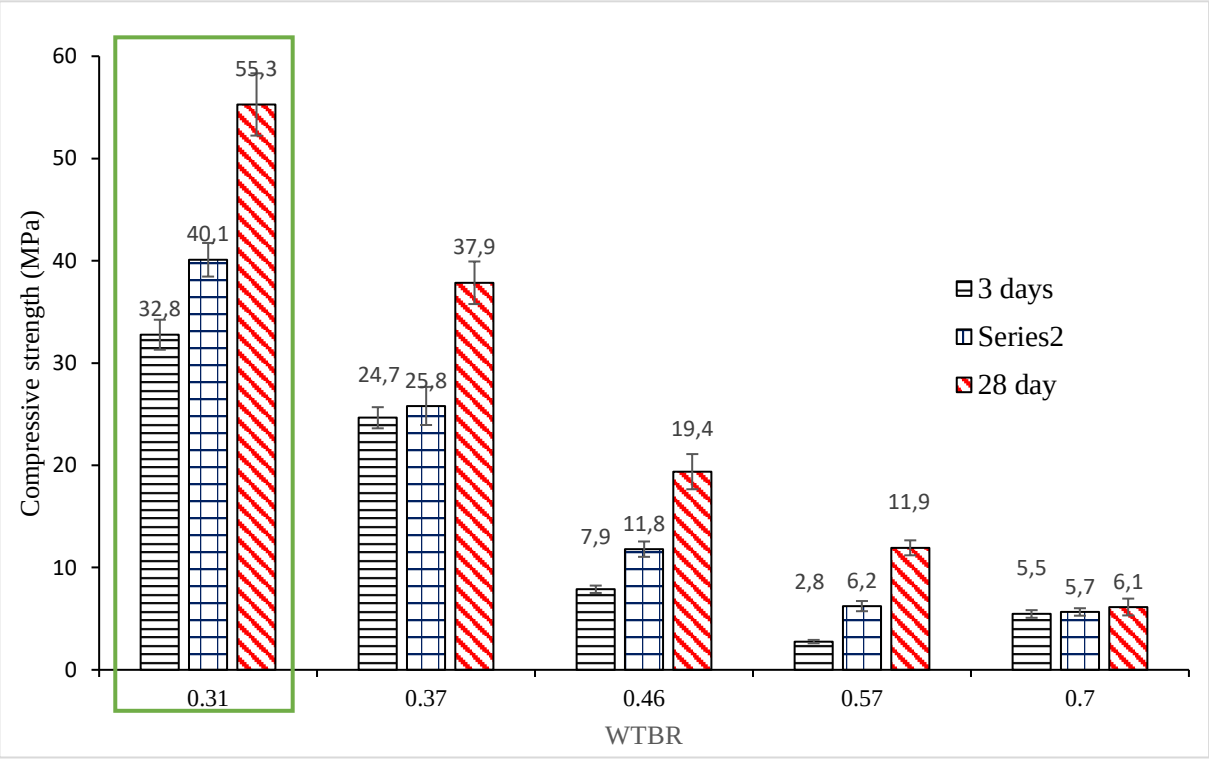

Figure 6.6 The effect on CS with aspect to WTBR calculated according to Equation 5.4. The ratios are SM (0.31), 0.37, 0.46, 0.57 and 0.70. the CS was measured for 3, 7 and 28 days

The decrease in CS with the addition of water is in line with the literature and is a result of that GP is not a hydrate so the water is not incorporated in the structure which means the more water the less material to form polymers with. The samples of 0.70 WTBR also suffered shrinking during drying can be seen in *Appendix F*. These samples were also noticeably lighter something that could be correlated to the larger porosity seen in *Figure 6.12*. Comparing the low performing samples in this test to the low performing sample in *Figure 6.5* the samples with more water do not show the same increase in CS with time compared to the 20°C sample. The small amount of water added between 0.31 and 0.37 gives rise to a decrease of 31% of CS.

6.3.2.3 Sodium silicate content

In *Figure 6.7* the result of changes in the amount of SoSi is shown. For all samples, the water amount, GW, and MM was same, the only thing that was changed was the amount of SoSi. The method of curing was 24h at 60°C then demould and left to dry in ambient temperature and moisture until CS testing.

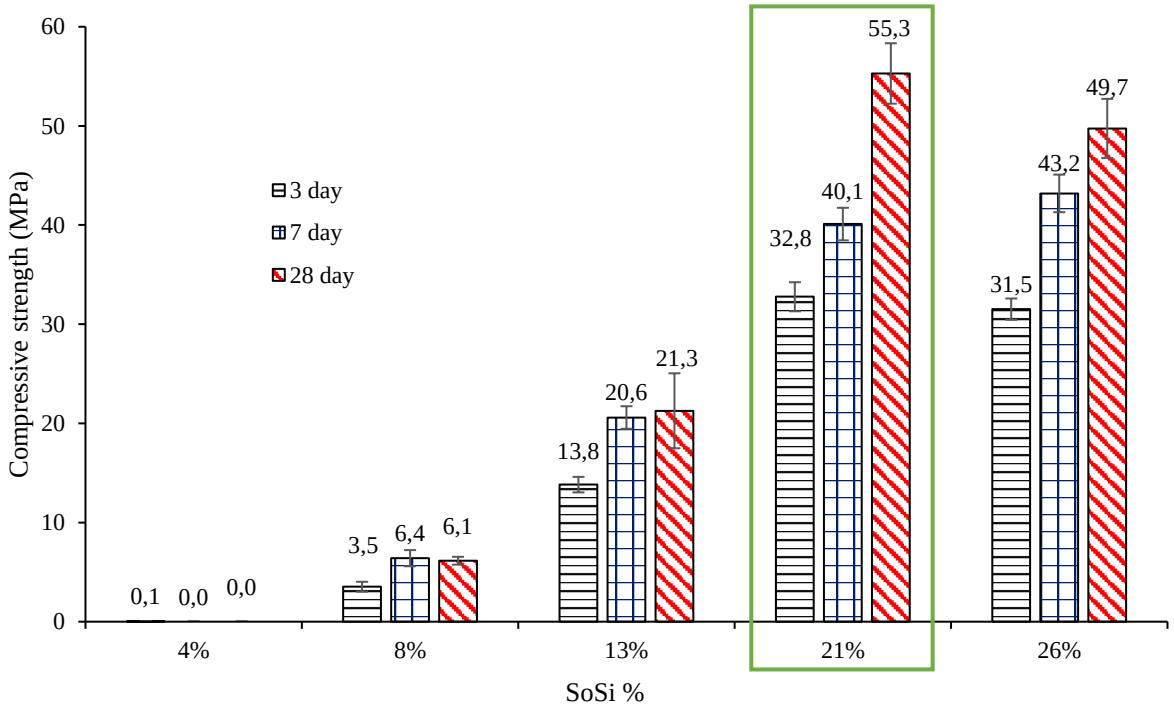

Figure 6.7 The effect on CS for the amount of SoSi used. The percentage is calculated as Equation 5.3. 21% is the SM. (For 4% only a 3-day test was done, the samples did not form cubes and fell apart upon touching see Appendix G)

The CS is increasing with an increasing amount of SoSi up to at least 21%. The results for 4% was non existing since the samples did not create a paste but rather several small pellets that when dried fell apart. After the 3 days test these samples were excluded from the experiment (all samples can be seen in *Appendix G*). Samples containing 26% of SoSi had a lower CS then those with 21%. According to the literature a CS over 20 MPa is desired for OPC so to compete with OPC a minimum of 13% would be required.

The difference between 21% and 26 % is not large enough to say that there is a difference, so it would be reasonable to assume that the maximum solubility of the SoSi used is somewhere around 21%. This would explain the stagnation of the CS increase around that percentage.

When mixing the samples the paste got progressively wetter with the amount of SoSi added this can be seen in *Appendix G* with the sample with the least SoSi not being able to forma a paste and that the cavities in the samples due to not filling out the moulds got smaller and smaller as the amount of SoSi increased and the paste was self-compacting. This phenomenon of getting a wetter paste the more powder added arises from the 16% of water in the SoSi. This means that the sample with the most SoSi also contained 15g more water. And even though the WTBR was higher for the dryer sample the fact that a small amount of water can make a large difference is visible in *Figure 6.6* where the increase of 20g (0.31-0.37 WTBR) lead to a reduction of 30%

When measuring the effects of WTBR on GP as well as the SoSi amount difficulties separating the tests emerges. When changing the WTBR the concentration of SoSi is inadvertently changed as well. The ratio between binder and SoSi does not change but the concentration of the SoSi in relation to water changes. This is not desired since a constant concentration of SoSi in water is needed to compare to two-part GP. To combat this more SoSi could be added but then the ratio between SoSi and binder will change. To investigate the true relation between these two parameters another experimental set up than the one used here is needed.

6.3.2.4 Shorter curing time

To keep manufacturing energy consumption and production costs at a minimum, a reduction of the curing time would be an interesting alternation to the process. The result of these test can be seen in *Figure 6.8*. The samples 60°C_4h and 60°C_24h is a comparison between 4h and 24h curing for a sample with SM composition as can be seen from the green square. The 24h sample exhibits a much larger CS for all measurements compared to 4h curing. The same trend can be seen between samples 80°C_4h and 80°C_24h.

When comparing the 4h tests for the SM it is visible that the 80°C samples is stronger than the 60°C. Almost reaching the same CS 60°C as for 3 days within the first hour of drying.

A comparison between samples 60°C_4h_BP and 60°C_24h_BP gives that the curing of 4h is better for a samples prepared using the BP composition at 28 days but has a lower CS at 7 days. When comparing the different temperatures for curing the BP for 4h it is observed that 60°C is stronger at late-stage testing while 80°C has a higher CS within the first hour of drying. Measurements for 24h BP 3-day testing is missing.

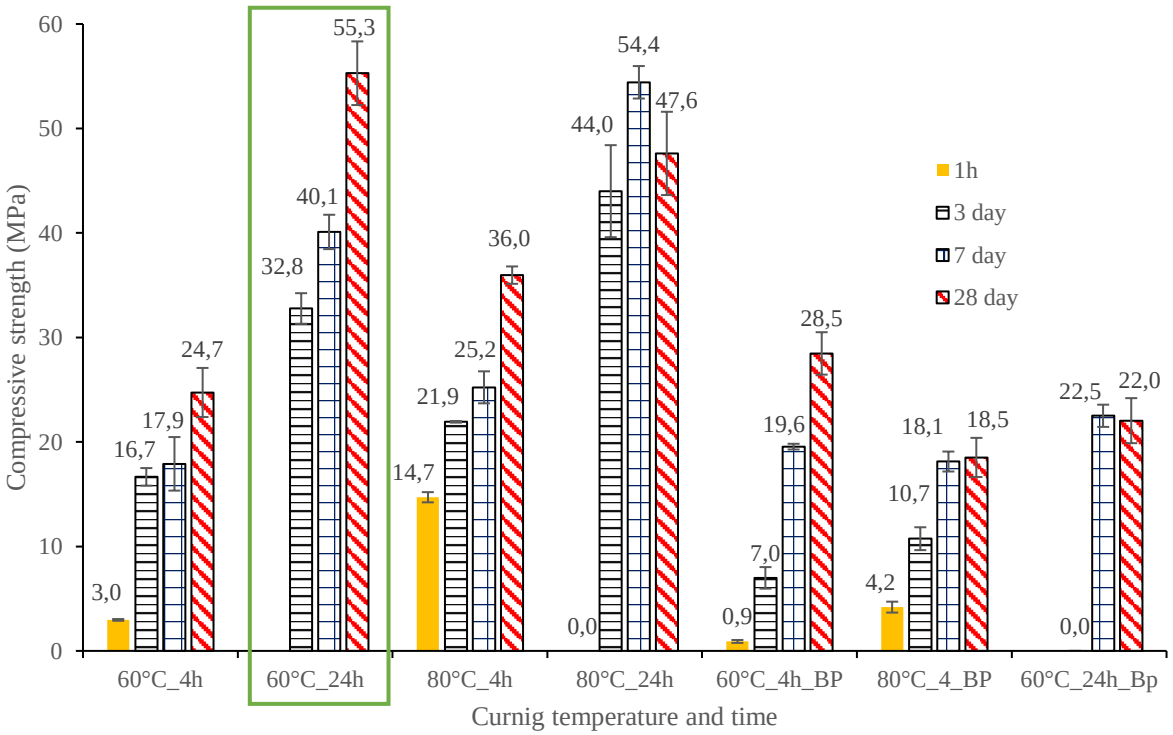

Figure 6.8 Graphs with comparisons between 4 and 24h curing in different temperatures for different water content geopolymer pastes.

The highest CS is reached for the SM but when comparing the different temperatures for the SM composition and 4h curing the 80°C the 80°C is the best. This means that to lowered the curing time for a GP the temperature can be increased. This would result in higher late-stage CS as well as good properties already after 1h of drying. This can be supported by the RK graph in *Figure 6.9* where the 80°C has a higher peak value above the Ref and the 60°C samples does not pass it in elevated temperature until long after 4h meaning that the 80°C sample would benefit from a shorter cuing time.

When the WTBR is increased for the BP the early-stage results are the same, with low performance for 60°C while although not rivalling the SM the 80°C BP is stronger at this temperature than for 60°C. When let to dry the 60°C BP passes the 80°C BP at about 7 days and will have a higher CS for 28 days test. This contradicts the data form the SM. The possibility of lowering the curing time to 4h is plausible. However, the WTBR and curing temperature should be altered to fit the intended porous of the GP.

6.4 Reaction kinetics

The reaction kinetics from the experiments were compiled into different graphs depending on the parameter analysed. Since the method described in section *5.3.1* can be used to verify and quantify the reaction of GP, the method will be compared to the CS of the samples to see if any correlations between RK and the CS can be found

6.4.1 Results for curing temperature

In *Figure 6.9a* the data from the temperature experiment is presented. From this data, it is visible that the temperature in the samples has been higher than the reference temperature for temperatures exceeding 40°C. To easier see the difference from each reference the differential between the sample and the reference was calculated and plotted in *Figure 6.9b*.

The graph for 20°C increased in temperature above the reference alongside the other samples, but decreased in temperature after 45 min. To be equal to the reference at 150 min.

The graph for 40°C follows the reference samples at all points. No elevated temperature compared to the Ref can be observed in *Figure 6.9a*. In *Figure 6.9b* the deviation from the Ref is below 2°C.

The 60°C samples temperature clearly deviates from the Ref, in *Figure 6.9a* the graph is starting to depart form the Ref graph during the time before the samples has reached the oven temperature of 60°C. after around 150 min the peak value above Ref is registered and from *Figure 6.9b* it can be determined to 5.3°C above Ref. the temperature decreases some and stabilizes at 2.5°C above Ref from 400 mins for the duration of the experiment.

For 80°C the graph is similar to that of 60°C with the exception that it from *Figure 6.9a* looks to be a bit slower to exceed the Ref temperature, this is however not confirmed by *Figure 6.9b.* where 80°C looks to have a higher differential than 60°C. 80°C reaches a higher temperature above Ref of 7°C, but then settles at the same differential temperature as 60°C.

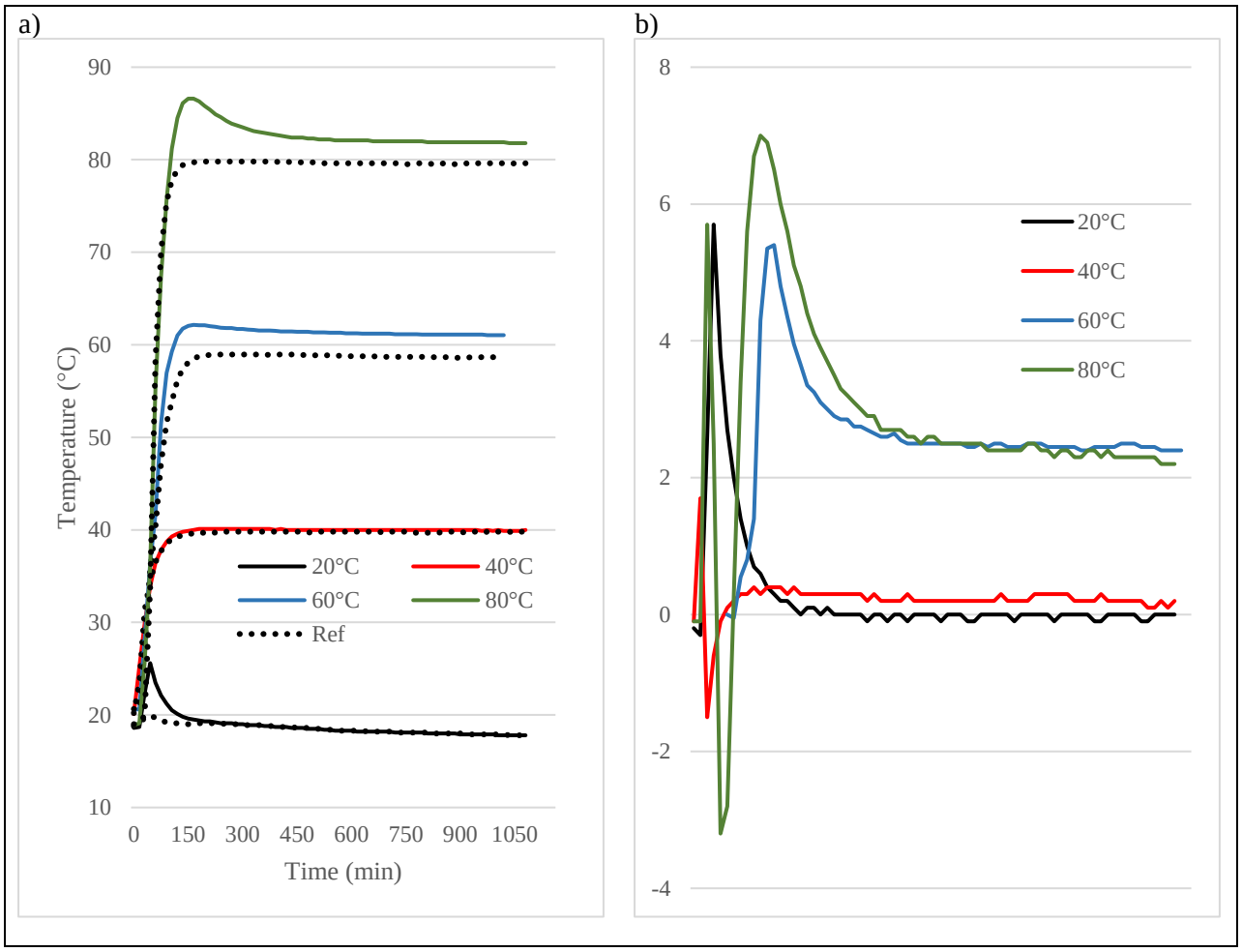

Figure 6.9 a) is The RK of the different temperatures 20°C (black), 40°C(red), 60°C(blue) and 80°C(green). b) the temperature difference between the sample and the reference for each sample in a).

The rapid increase in temperature for 20°C at the beginning is interesting since the other samples can not exhibit this increase since the environment of the oven is warmer than that increase. This increase could be some exothermic dissolution reaction of the SoSi or an actual GP reaction. An exothermic dissolution could be possible and non-detectible in the other samples due to the increasing temperature form their environments.

The small difference between the reference and the samples below 40°C could be due to that the heat created form the reaction is transferred to the environment faster than it is created from the reaction. When the temperature is increased so is the rate of reaction which lead to more heat being released. This could be why 80°C has a higher peak value than 60°C.

The comparison to CS of the same samples the CS of 60°C and 80°C are similar in CS and are similar in RK. The same can not be said about the 20°C and 40°C samples these have a large difference in the 3-day test which would be the one most affected by the curing regime. This could be an effect of the fact that the temperature increase for these samples over the Ref could be set equal to zero since it is below 1°C.

6.4.2 Results for WTBR

The same measurements were done for the sample series where the effect of WTBR was investigated. The graphs can be seen in *Figure 6.10a*, with a range from the SM (0.31) to the highest WTBR of 0.70.

All these samples were, as previously stated cured at 60°C for 24h. The full 24h is not included in the graph since the differences from the reference were stagnant from the cut off time (19h) until 24h. These curves correspond to the CS in *Figure 6.6*.

In *Figure 6.10a* it is difficult to see any differences between the samples, especially when the temperature is settling after 500 min. From *Figure 6.10b* the difference is more apparent. The SM sample reaches the highest temperature and also remains the highest above Ref. The second highest sample is 0.57 followed by 0.37. these samples seem to be very similar in temperature development. Then the 0.46 sample differentiates some from the Ref to return to below 1°C above Ref. For the 0.70 sample it never has a peak above the Ref but just settles on a temperature less than 1°C above the ref.

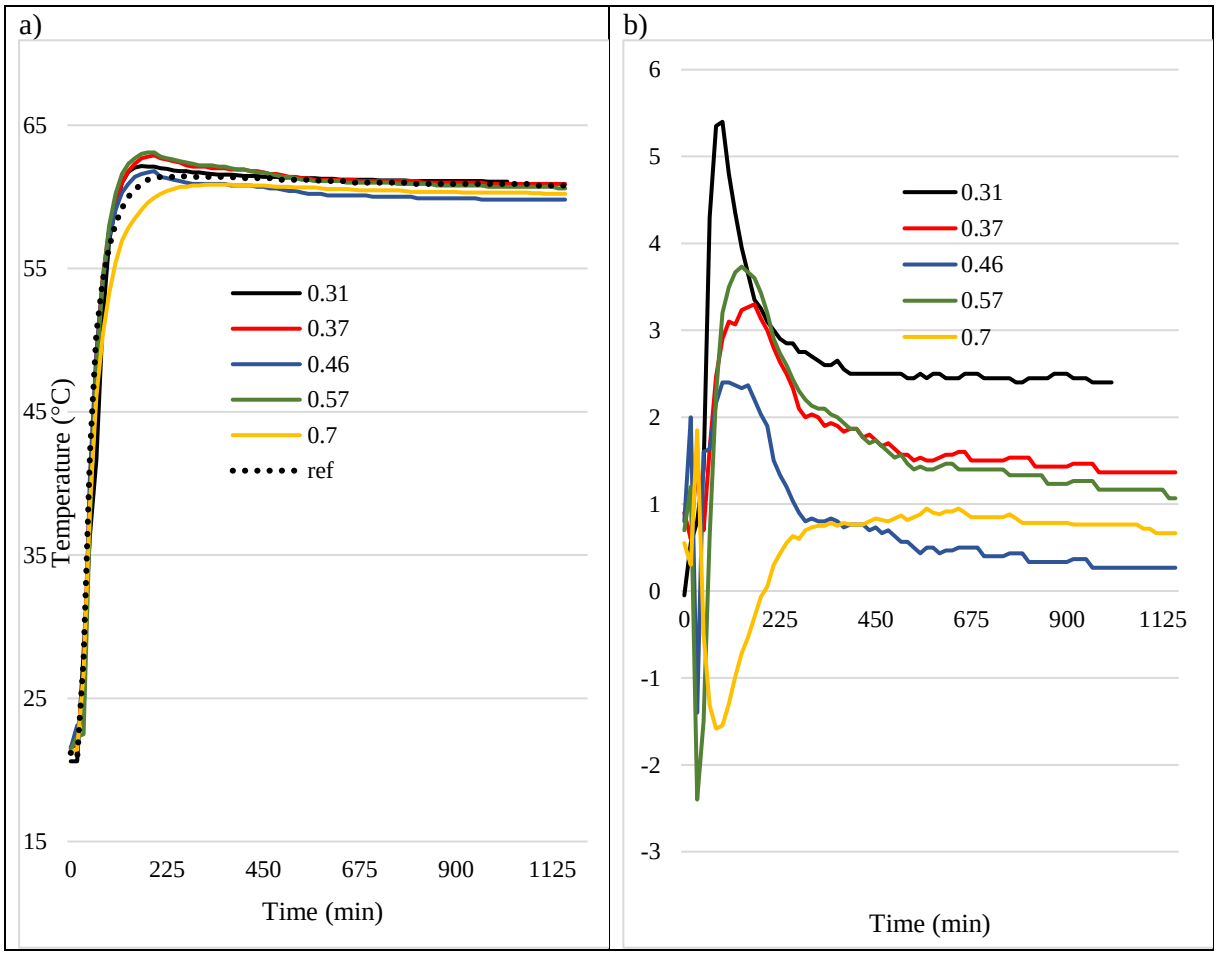

Figure 6.10 a) the RK of the different WTBR examined SM(black), 0.37(red), 0.46(blue), 0.57(green) and 0.70(yellow). b) is the difference between sample and reference for the samples in a.

When comparing the results of the RK with the CS for WTBR the results of the RK is surprizing. From RK, 0.57 would have a CS higher than 0.46 however this is not the case, there is an increase of 60% when reducing the WTBR from 0.57 to 0.46.

This indicates that the results form RK is not suitable to make precise predictions on the CS. It can make some broad suggestions that a high WTBR would have a low CS and the opposite for a low WTBR. To keep in mind when comparing the result form RK with the CS is that the change in percentage of CS is large between 0.46,0.57 and 0.70 WTBR but the real numbers is not that large which might be the reason why RK is not able to detect a difference. The difference between them is not significant enough.

6.4.3 Results for SoSi amount

In *Figure 6.11a* the sample with 26% of alkali has the highest temperature peak followed by 21% and 13%, with 4% and 8% barely increasing the temperature above the Ref. When comparing to *Figure 6.11b* all samples have a high elevated temperature before 60 min. This gives the impression that all samples exhibit a large exothermic reaction. The reality can however be seen in *Figure 6.11a* where all samples have a higher temperature than the Ref before reaching 60°C. this could be because the ref contained a larger amount of water which would make it increase in temperature slower than the other samples. Resulting in a high differential temperature before reaching oven temperature.

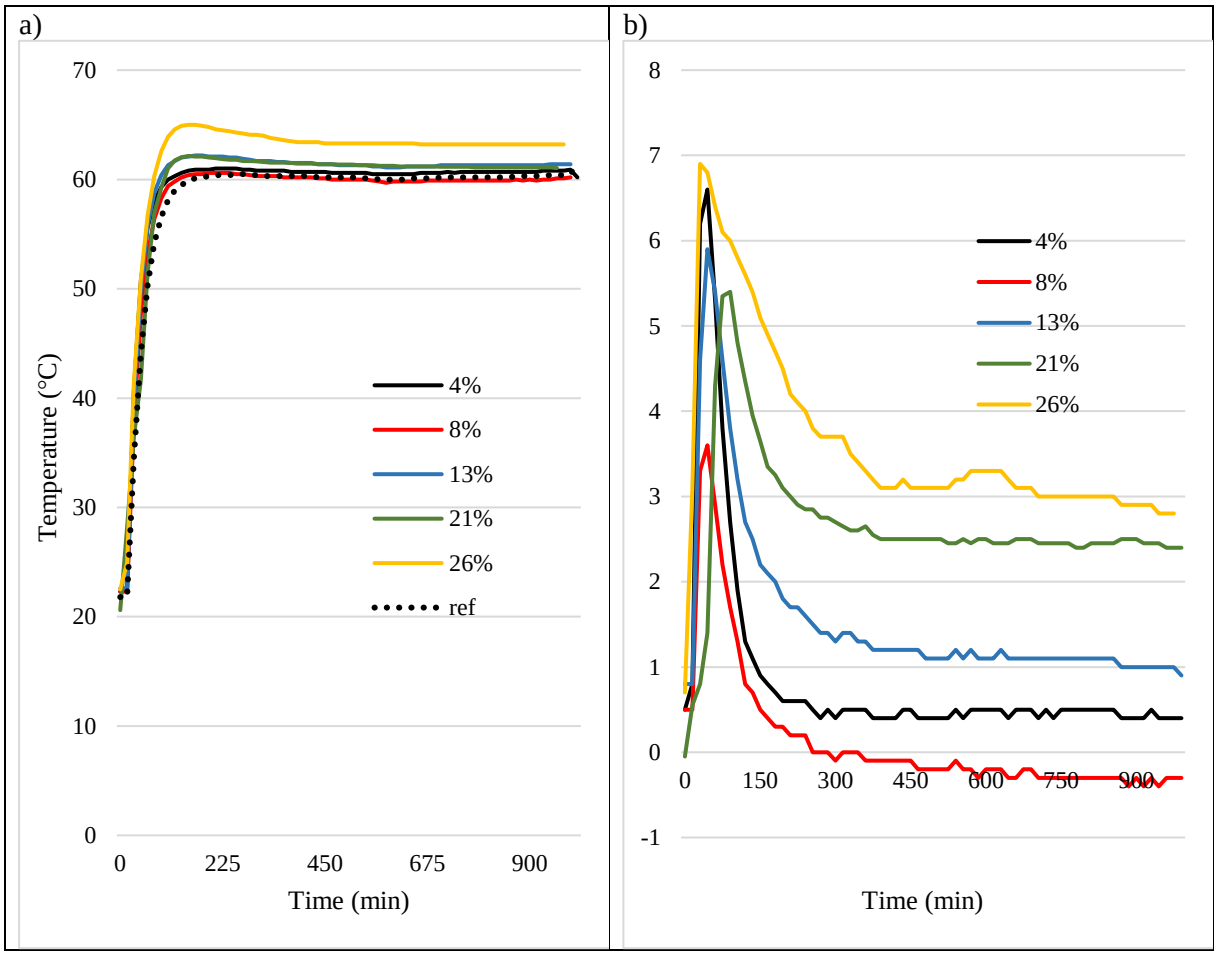

Figure 6.11 a) the RK for the different amounts of SoSi used in different samples SM(Green), 4%(Black), 8%(Red), 13%(Blue) and 26%(Yellow). Calculated according to Equation 5.3 b) is the difference between the samples and Ref in a).

The different SoSi contents resulted in different RK, again these values did not match the CS for each sample. But as a broad method to get an indication on the effect of SoSi content on the CS it could work. But not when comparing individual samples

The method of determining the quality of the GP using the set up described in *section 5.3.1* had some limitations. From literature the initial peak value over the Ref took longer time to form than what had been described in literature. This might had been prevented by utilizing a narrower sampling of temperatures. Sampling the temperature every 15 min might had been to infrequently. Since the literature stated a peak at around 30 min where this setup only had measured two measurements. The employment of some kind of bath water or oil could had decreased the time to reach the desired temperature, which could had improved the method. Something that the method was able to predict was

the order of CS by comparing the long-term differential temperature above the Ref. By only using this temperature differential the method could be used to give a rough estimate on the CS.

6.5 Microscopy

The porosity influences a lot of properties of the GP, such as water resistance, chemical resistance, mechanical properties, and protection against freeze damage. One sample prepared with as SM in two moulds came out of the oven looking strikingly different *Figure 6.12a* and *Figure 6.12b*. as can be seen a) was smooth while b) was rough. Both samples had been treated the same but came from different moulds. All samples in each mould looked the same. One mould smooth one rough. These samples where investigated under a microscope to see if there was any differences in the porosity, i.e. the structure on the outside had continued on the inside. Column three of *Figure 6.12* is pictures of a sample with WTBR of 0.70.

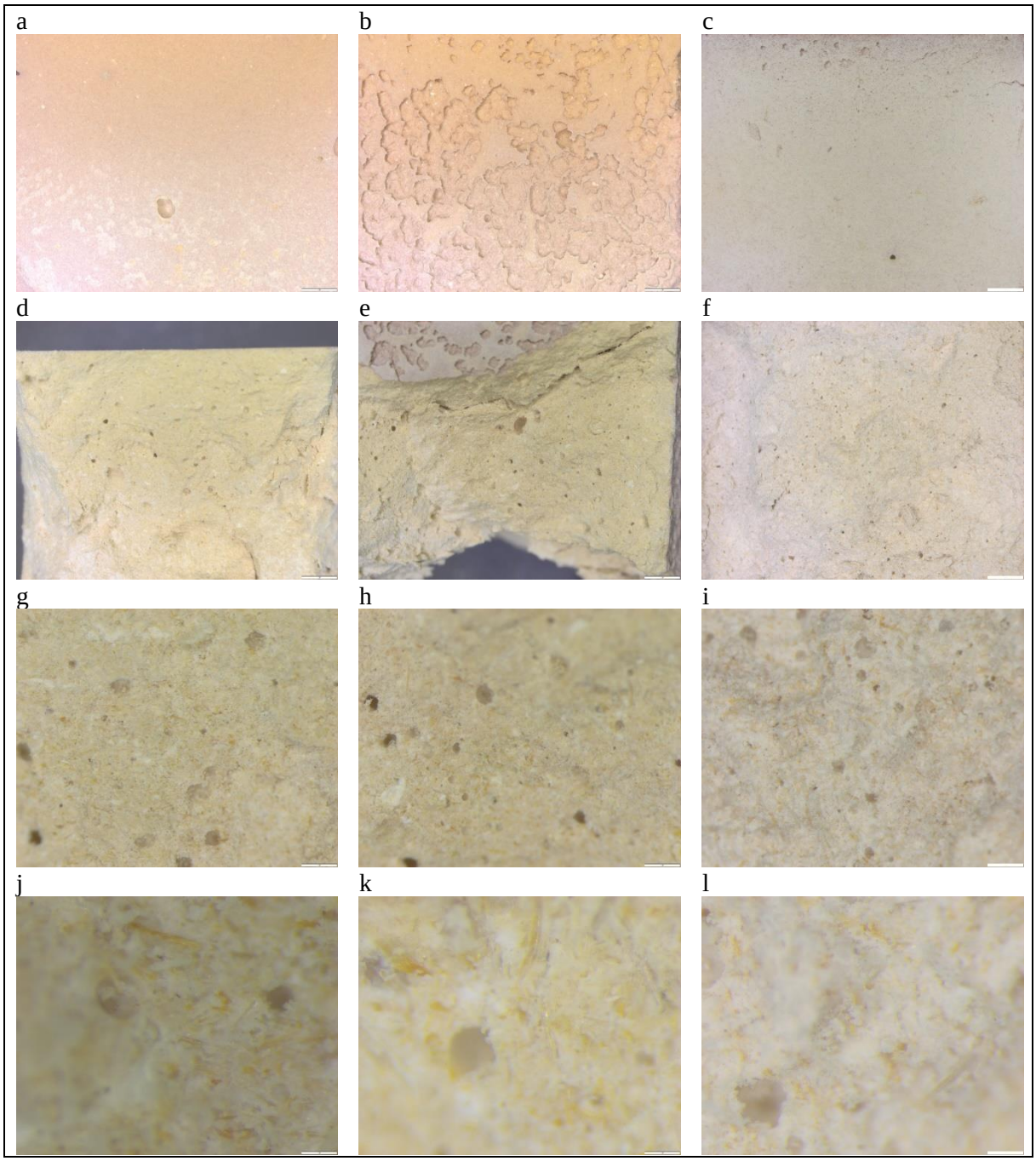

Figure 6.12 Colum 1. is SM cured for 24h at 60C with a smooth surface, column 2 SM cured for 24h at 60C with a rough surface, column 3 has WTBR 0.40 cured for 24h at 60C. Row 1 zoom 7x, row 2 zoom 7x, row 3 zoom 34x, row 4 zoom 115x.

When comparing *Figure 6.12d* and *Figure 6.12e* the radical difference from the outside is no longer as telling. The sample of the rough cube still exhibits a bit more porosity than the smooth sample. When moving closer and looking at *Figure 6.12g* and *Figure 6.12h* the difference is no longer visible. If anything, the smooth sample seems to be more porous.

This way of measuring porosity on one sample with an easy setup does not give the full picture of the actual relationship between roughness of the surface and the porosity of the sample. Nonetheless, the striking difference of the outside did not seem to translate to the inner structure of these samples. To find out what caused the difference between the moulds more research is needed.

7 Conclusion

The results from TGA show that the largest impact on the mass loss when heated comes from the water trapped in the structure as free water. This water is not included in the structure since most of it leaves before 100°C. This indicates that the samples do consists to a large degree of GP and not AAM since the hydrate structure of AAM would release more water between 100°C and 300°C. The samples do reduce their mass in this interval but since the pure GW has a decrease due to the phenolic binder this decrease would be a combination of phenolic binder and some AAM formed.

The XRD affirms the amorphous structure although some crystallinity is found in the samples. This is not surprising since the geopolymerization is a surface reaction that retains a lot of the original structures of the raw materials something that also can be seen in the XRD where some crystalline phases are transferred from the raw materials to the samples. The presence of crystalline phases that appear in the samples that can not be found in the raw materials needs more research to determine the origin and structure.

The use of the reaction kinetics measurement as an indicator of the quality of the GP was limited. The measurement seemed too inaccurate to be able to give a good prediction in the CS of the GP. For elevated temperature, the RK showed promising results with a temperature well above the reference. However, the height or even the integrated temperature could not predict the CS well enough to know the characteristics of the sample before testing. The method also lacked the ability to show an increase in temperature for temperatures below 40°C. The reaction was happening but the heat release to the environment was higher than the production of heat from the reaction.

The temperature experiment concludes that the most advantageous curing temperature for geopolymers with the composition of SM is 60°C. For lower temperatures, the compressive strength lowers significantly.

The alteration of the WTBR for the samples concludes that for samples cured for 24h at 60C the highest CS is consistent with the lowest water amount. However, to produce a paste that can be easily moulded with the least effort a WTBR of 0.43 is preferable

For sodium silicate amount the choice of the amount is related to the cost of the material. More sodium silicate gives higher compressive strength until a cut off between 21% and 26%. The concentration should exceed 13% to produce a geopolymer with properties comparable to OPC.

To reduce the production time and energy consumption a reduced curing time could be utilized, but to retain good properties a recommended curing temperature of 80°C is advised. If a paste with 0.43 WTBR is used the choice of temperature needs to include the importance of early-stage CS into account, since this is drastically altered by changing the curing temperature.

8 Future work

The continuations on this work would be a narrower set of samples to find cut off points in the water to binder ratio and sodium silicate use. The system of geopolymers is highly sensitive to changes in the water to binder ratio. Therefore, a closer span of samples would hypothetically yield a drastic cut off point where the compressive strength is kept high while the processability is preserved. The same could be done for the sodium silicate amount.

More research is required to find the relation between alkali and water. Since these are closely connected and affect each other when changed a better experimental setup is needed to fully concretise the impact that these two parameters have on the compressive strength of a geopolymer.

This project only looked at the binder itself, further studies should be made on adding a filler material to the binder. Investigations on the maximum filler capacity for the geopolymer, for different applications. How would other silica-based materials work such as rocks or sand for volume increasing filler? And look at fibres to lighten the material. Such as Styrofoam beads or different kinds of lightweight fibres.

9 References

Abdullah, M. M. A. B., Ming, L. Y., Yong, H. C., & Tahir, M. F. M. (2018). Clay-Based Materials in Geopolymer Technology. In. InTech. https://doi.org/10.5772/intechopen.74438

Andrew, R. M. (2018). Global CO2 emissions from cement production. *Earth System Science Data*, *10*(1), 195-217. https://doi.org/10.5194/essd-10-195-2018

Ardebili, M. A. H., & Mirzabozorg, H. (2010). Numerical simulation of reservoir fluctuation effects on the nonlinear dynamic response of concrete arch dams.

Chi, M. (2017). Effects of the alkaline solution/binder ratio and curing condition on the mechanical properties of alkali-activated fly ash mortars. *Science and Engineering of Composite Materials*, *24*(5), 773-782. https://doi.org/10.1515/secm-2015-0305

Cong Ma, G. L., Ye Shi, Youjun Xie. (2018). Preparation of cleaner one-part geopolymer by investigating different types of commercial sodium metasilicate in China. *Journal of Cleaner Production*, *201*, 636-647.

Constructor, T. (2007). *Stress Strain Curve for Concrete*

Das, S. K., & Shrivastava, S. (2021). Influence of molarity and alkali mixture ratio on ambient temperature cured waste cement concrete based geopolymer mortar. *Construction and Building Materials*, *301*, 124380. https://doi.org/10.1016/j.conbuildmat.2021.124380

Davidovits, J. (2020). *GEOPOLYMER Chemistry & Applications* (5th ed.). Institut Géopolymère.

De Jong, B. H. W. S., & Brown, G. E. (1980). Polymerization of silicate and aluminate tetrahedra in glasses, melts, and aqueous solutions—I. Electronic structure of H6Si2O7, H6AlSiO71−, and H6Al2O72−. *Geochimica et Cosmochimica Acta*, *44*(3), 491-511. https://doi.org/10.1016/0016-7037(80)90046-0

Dietmar Gross, W. H., Jörg Schröder, Wolfgang A. Wall, Javier Bonet. (2011). *Engineering Mechanics 2*. Springer Heidelberg Dordrecht London New York. https://doi.org/DOI 10.1007/978-3-642-12886-8

Duxson, P., Mallicoat, S. W., Lukey, G. C., Kriven, W. M., & Van Deventer, J. S. J. (2007). The effect of alkali and Si/Al ratio on the development of mechanical properties of metakaolin-based geopolymers. *Colloids and Surfaces A: Physicochemical and Engineering Aspects*, *292*(1), 8-20. https://doi.org/10.1016/j.colsurfa.2006.05.044

Duxson, P., Provis, J. L., Lukey, G. C., Mallicoat, S. W., Kriven, W. M., & Van Deventer, J. S. J. (2005). Understanding the relationship between geopolymer composition, microstructure and mechanical properties. *Colloids and Surfaces A: Physicochemical and Engineering Aspects*, *269*(1-3), 47-58. https://doi.org/10.1016/j.colsurfa.2005.06.060

E. Petrakis, V. K., K. Komnitsas (2019). Effect of Particle Size on Alkali-Activation of Slag. *International Journal of Materials and Metallurgical Engineering 13*(9), 471-474.

Hardjito, D., Wallah, S. E., Sumajouw, D. M. J., & Rangan, B. V. (2005). Fly Ash-Based Geopolymer Concrete. *Australian Journal of Structural Engineering*, *6*(1), 77-86. https://doi.org/10.1080/13287982.2005.11464946

He, P., Wang, M., Fu, S., Jia, D., Yan, S., Yuan, J., Xu, J., Wang, P., & Zhou, Y. (2016). Effects of Si/Al ratio on the structure and properties of metakaolin based geopolymer. *Ceramics International*, *42*(13), 14416-14422. https://doi.org/10.1016/j.ceramint.2016.06.033

Horvat, B., & Ducman, V. (2020). Influence of Particle Size on Compressive Strength of Alkali Activated Refractory Materials. *Materials*, *13*(10), 2227. https://doi.org/10.3390/ma13102227

Hyunjung Kim, Y. K. (2012). *Characteristics of the Geopolymer using Fly Ash and Blast Furnace Slag with Alkaline Activators* 2012 4th International Conference on Chemical, Biological and Environmental Engineering, Singapore.

ISOVER, S.-G. (2022). *Glass Wool*. Retrieved 05-15 from Difference between geopolymers and alkali-activated materials)

J.M.G Cowie, V. A. (2007). *Polymers: Chemistry and Physics of Modern Materials* (3 ed.). CRC Press.

Kubba, Z., Fahim Huseien, G., Sam, A. R. M., Shah, K. W., Asaad, M. A., Ismail, M., Tahir, M. M., & Mirza, J. (2018). Impact of curing temperatures and alkaline activators on compressive

strength and porosity of ternary blended geopolymer mortars. *Case Studies in Construction Materials*, *9*, e00205. https://doi.org/10.1016/j.cscm.2018.e00205

Kushal Ghosh, P. G. (2018). Effect of Variation of Slag Content on Chemical, Engineering and Microstructural Properties of Thermally Cured Fly Ash-Slag Based Geopolymer Composites. *Rasayan Journal Chemistry*, *11*(1), 426-439.

Kühne, P. S. G. J. G. G. H. J. H. B. H.-C. (2016). Synthesizing one-part geopolymers from rice husk ash. *Construction and Building Materials*, *124*, 961-966. https://doi.org/https://doi.org/10.1016/j.conbuildmat.2016.08.017

Lemougna, P. N., Adediran, A., Yliniemi, J., Ismailov, A., Levanen, E., Tanskanen, P., Kinnunen, P., Roning, J., & Illikainen, M. (2020). Thermal stability of one-part metakaolin geopolymer composites containing high volume of spodumene tailings and glass wool. *Cement and Concrete Composites*, *114*, 103792. https://doi.org/10.1016/j.cemconcomp.2020.103792

Lemougna, P. N., Adediran, A., Yliniemi, J., Luukkonen, T., & Illikainen, M. (2021). Effect of organic resin in glass wool waste and curing temperature on the synthesis and properties of alkali-activated pastes. *Materials & Design*, *212*, 110287. https://doi.org/10.1016/j.matdes.2021.110287

Lesley E. Smart, E. A. M. (2005). *Solid State Chemistry An Introduction* (3 ed.). CRC press.

Li, Z., Zhang, W., Wang, R., Chen, F., Jia, X., & Cong, P. (2019). Effects of Reactive MgO on the Reaction Process of Geopolymer. *Materials*, *12*(3), 526. https://doi.org/10.3390/ma12030526

Luga, E., & Atis, C. D. (2016). Strength Properties of Slag/Fly Ash Blends Activated with Sodium Metasilicate and Sodium Hydroxide + Silica Fume. *Periodica Polytechnica Civil Engineering*, *60*(2), 223-228. https://doi.org/10.3311/ppci.8270

Luukkonen, T., Abdollahnejad, Z., Yliniemi, J., Kinnunen, P., & Illikainen, M. (2018). One-part alkali-activated materials: A review. *Cement and Concrete Research*, *103*, 21-34. https://doi.org/10.1016/j.cemconres.2017.10.001

Mo, B.-H., Zhu, H., Cui, X.-M., He, Y., & Gong, S.-Y. (2014). Effect of curing temperature on geopolymerization of metakaolin-based geopolymers. *Applied Clay Science*, *99*, 144-148. https://doi.org/10.1016/j.clay.2014.06.024

Mohammad I. M. Alzeer, H. N., Christopher Cheeseman, and Paivo Kinnunen. (2021). Alkali-Activation of Synthetic Aluminosilicate Glass With Basaltic Composition

Frontiers in Chemistry, *9*. https://doi.org/10.3389/fchem.2021.715052

NevadaReadyMix. (2022). *Testing the compressive Strenght of Concrete- What, why & how?* . Nevada ready mix Retrieved 05-15 from https://www.nevadareadymix.com/concrete-tips/testing-the-compressive-strength-of-concrete/

Patankar, S. V., Jamkar, S. S., & Ghugal, Y. M. (2013). Effect of Water-to-Geopolymer Binder Ratio on the Production of Fly ash Based Geopolymer Concrete. *international Journal of Advanced Technology in Civil Engineering 2*(1), 79-83.

Rakita, Y., Kedem, N., Gupta, S., Sadhanala, A., Kalchenko, V., Böhm, M. L., Kulbak, M., Friend, R. H., Cahen, D., & Hodes, G. (2016). Low-Temperature Solution-Grown CsPbBr3 Single Crystals and Their Characterization. *Crystal Growth & Design*, *16*(10), 5717-5725. https://doi.org/10.1021/acs.cgd.6b00764

Rashidian-Dezfouli, H., Rangaraju, P. R., & Kothala, V. S. K. (2018). Influence of selected parameters on compressive strength of geopolymer produced from ground glass fiber. *Construction and Building Materials*, *162*, 393-405. https://doi.org/10.1016/j.conbuildmat.2017.09.166

Rodríguez, M. T., & Pfeiffer, H. (2008). Sodium metasilicate (Na2SiO3): A thermo-kinetic analysis of its CO2 chemical sorption. *Thermochimica Acta*, *473*(1-2), 92-95. https://doi.org/10.1016/j.tca.2008.04.022

Sajjad Yousefi Oderji, B. C., Muhammad Riaz Ahmad, Syed Farasat Ali Shah. (219). Fresh and hardened properties of one-part fly ash-based geopolymer binders cured at room temperature: Effect of slag and alkali activators. *Journal of Cleaner Production*, *225*, 1-10.

Saludung, A., Ogawa, Y., & Kawai, K. (2018). Microstructure and mechanical properties of FA/GGBS-based geopolymer. *MATEC Web of Conferences*, *195*, 01013. https://doi.org/10.1051/matecconf/201819501013

Shoaei, P., Ameri, F., Karimzadeh, M., Atabakhsh, E., Zareei, S. A., & Behforouz, B. (2022). Difference between geopolymers and alkali-activated materials. In (pp. 421-435). Elsevier. https://doi.org/10.1016/b978-0-12-821730-6.00018-8

Shuntian Ouyang, W. C., Zongtang Zhang, Xinming Li, Wenfeng Zhu. (2020). Experimental study of one-part geopolymer using different alkali sources. *Journal of Physics: Conference Series*, *1605*. https://doi.org/10.1088/1742-6596/1605

Temuujin, J., Van Riessen, A., & Williams, R. (2009). Influence of calcium compounds on the mechanical properties of fly ash geopolymer pastes. *Journal of Hazardous Materials*, *167*(1-3), 82-88. https://doi.org/10.1016/j.jhazmat.2008.12.121

Various structural linkage schemes in silicates. (2022). In: Encyclopeadia Britannica.

Woellner. (2015). Silkalon A. In *Sodium Disilicate Powder*. Ludwigshafen.

Yliniemi, J., Kinnunen, P., Karinkanta, P., & Illikainen, M. (2016). Utilization of Mineral Wools as Alkali-Activated Material Precursor. *Materials*, *9*(5), 312. https://doi.org/10.3390/ma9050312

Yuksel, I. (2018). Blast-furnace slag. In (pp. 361-415). Elsevier. https://doi.org/10.1016/b978-0-08-102156-9.00012-2

Zhijun He, X. Z., Junjie Wang, Mulan Mu, Yuli Wang (2019). Comparison of CO2 emissions from OPC and recycled cement production. *Construction and Building Materials*, *211*, 965-973. https://doi.org/https://doi.org/10.1016/j.conbuildmat.2019.03.289

10 Appendix

Appendix A

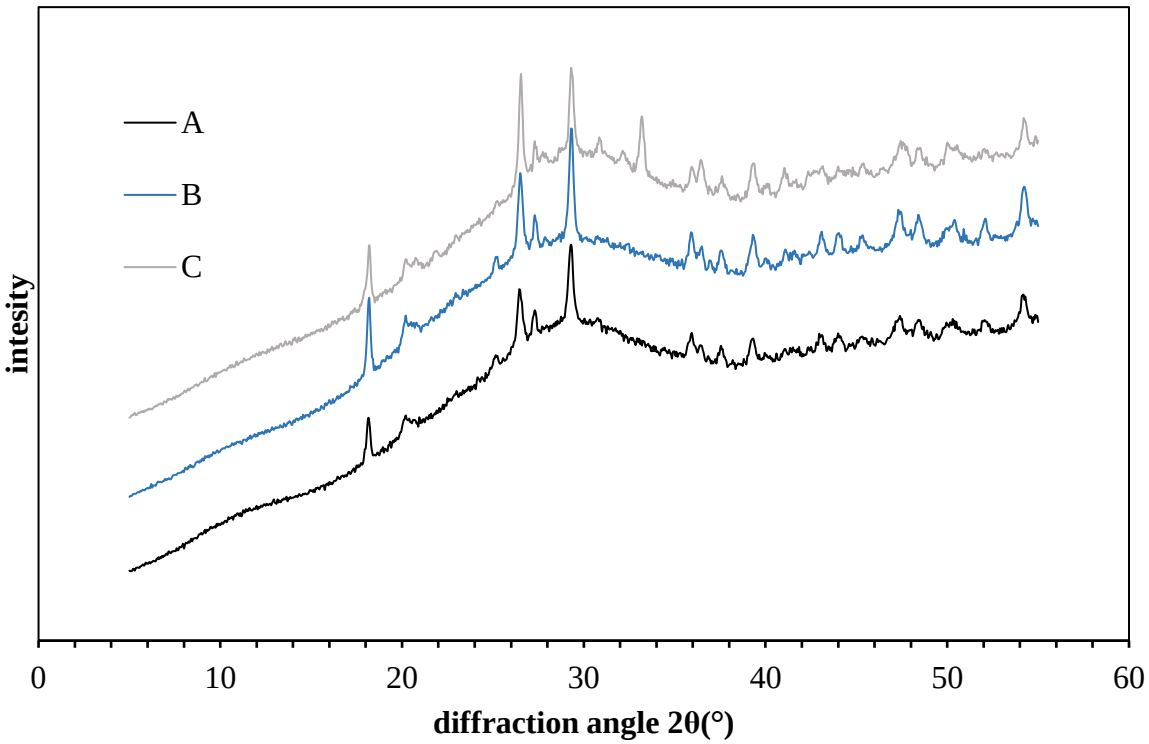

Appendix A closer XRD comparison of sample A B and C, than what can be seen in Figure 6.1

Appendix B

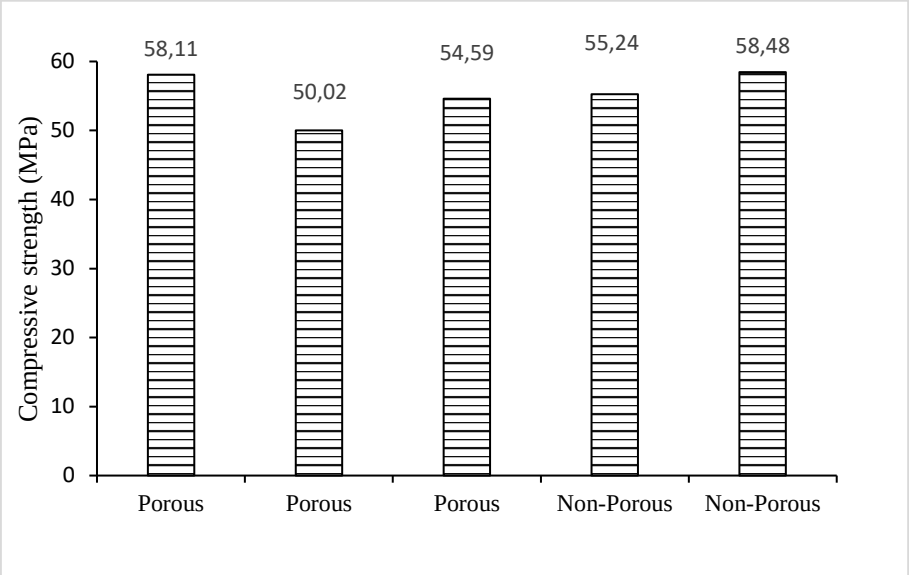

Appendix B Compression for smooth and rough surfaces for 28 days of SM samples with 24h curing at 60°C

Appendix C

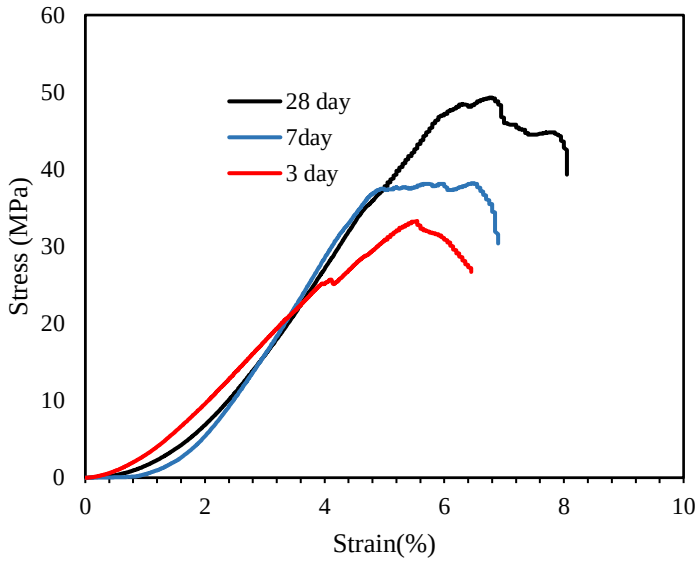

Appendix C Comparison between the behaviour of the geopolymer for 3,7 and 28 days of rest after curing. For SM cured for 24h at 60°C

Appendix D

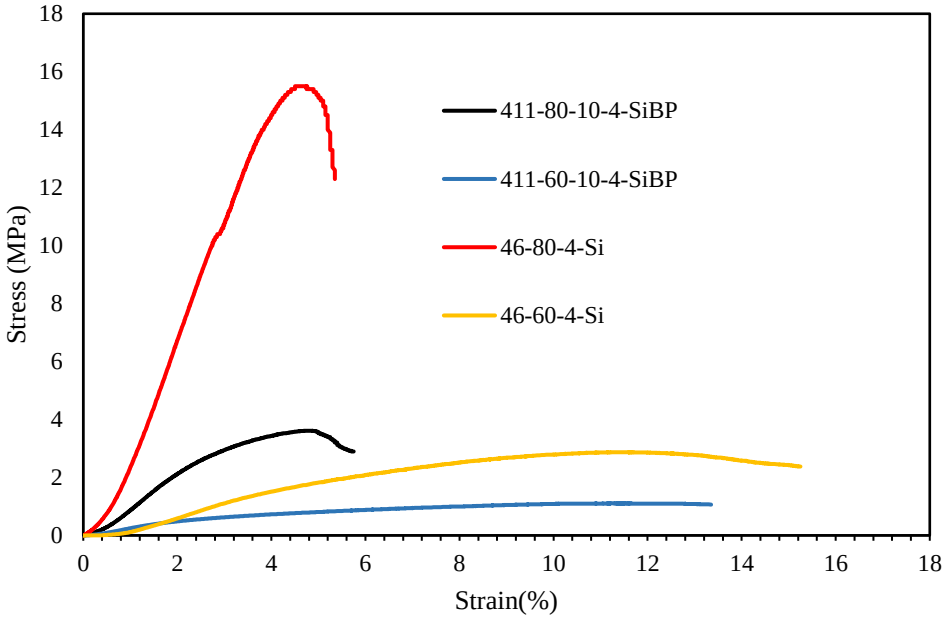

Appendix D A comparison between stress-strain curves for different WTBR and temperatures

Appendix E

Appendix E Samples cured at different temperatures from the left: 20°C, 40°C, 60°C and 80°C

Appendix F

Appendix F Samples of different WTBR from the left 0.31, 0.37, 0.46, 0.57, 0.7

Appendix G

Appendix G Samples with different SoSi content from the left, 4%, 8%, 13%, 21% and 26%

LUND
UNIVERSITY

LTH

FACULTY OF
ENGINEERING